Beyond a PeV – Particle acceleration to extreme energies in cosmic sources
Institut d'Astrophysique de Paris, September 13-16, 2016

Formation dynamics of nonrelativistic collisionless shocks: particle-in-cell simulations and analytical modeling

L. Gremillet[1], C. Ruyer[1,2]
[1]CEA, DAM, DIF, F-91297, Arpajon, France
[2]SLAC National Accelerator Laboratory, Menlo Park, USA

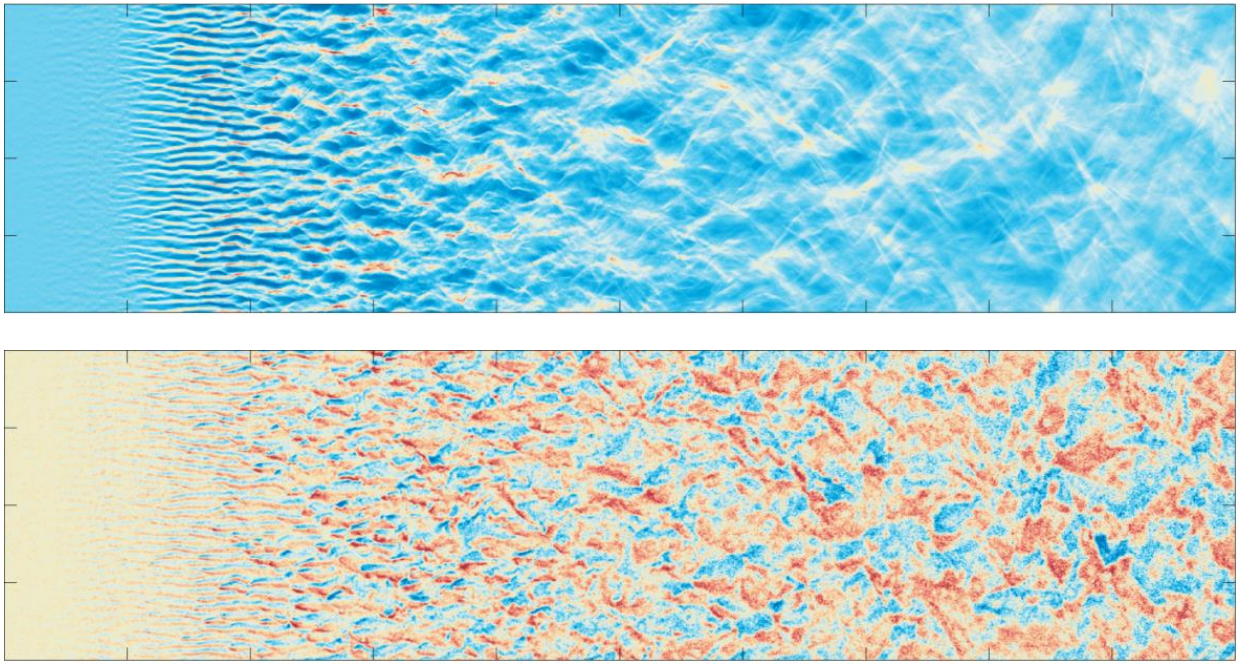

Weibel instability-induced collisionless shocks may explain various high-energy astrophysical phenomena

- Collisionless turbulent shocks are held responsible for energetic particle and radiation generation in powerful space environments (supernovae remnants, gamma-ray bursts, pulsar wind nebulae…)[1]

- The Weibel instability[2] seems to be a key player for shock formation in non/weakly magnetized settings[3,4]:
  - develops in counter-streaming and/or anisotropic plasmas;
  - generates magnetic micro-turbulence which dissipates the flow kinetic energy;
  - provides scattering centers causing Fermi-type particle acceleration and high-energy radiation emission.

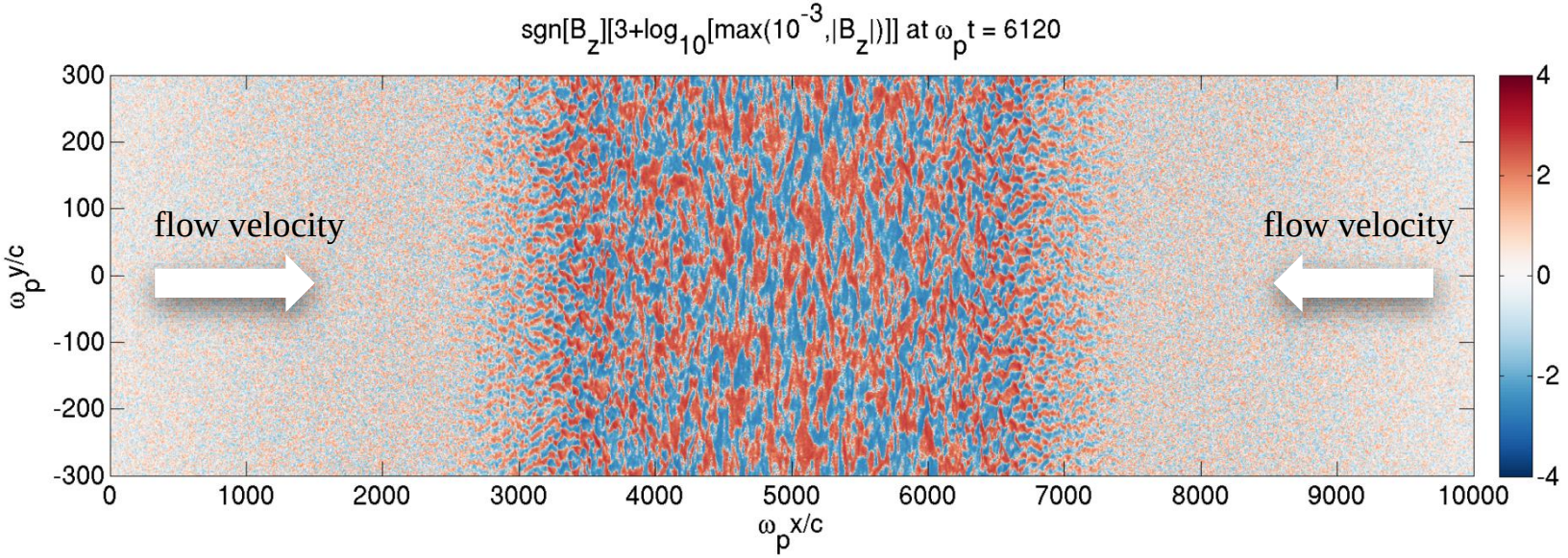

[1]T. Piran, RMP **76**, 1143 (2005); M. Lemoine *et al.*, ApJ **645**, L129 (2006).
[2]E. S. Weibel, PRL **2**, 83 (1959); M.V, Medvedev & A. Loeb, ApJ **526**, 697 (1999)
[3]A.Spitkovsky, ApJ **682**, L5 (2008); L. Sironi *et al*, ApJ **726**, 1 (2011)
[4]A. Stockem *et al.*, Sci. Rep. **4**, 3934 (2014)

Standard scenario of turbulent shock formation in Weibel-unstable colliding plasmas

CALDER PIC simulation[1]

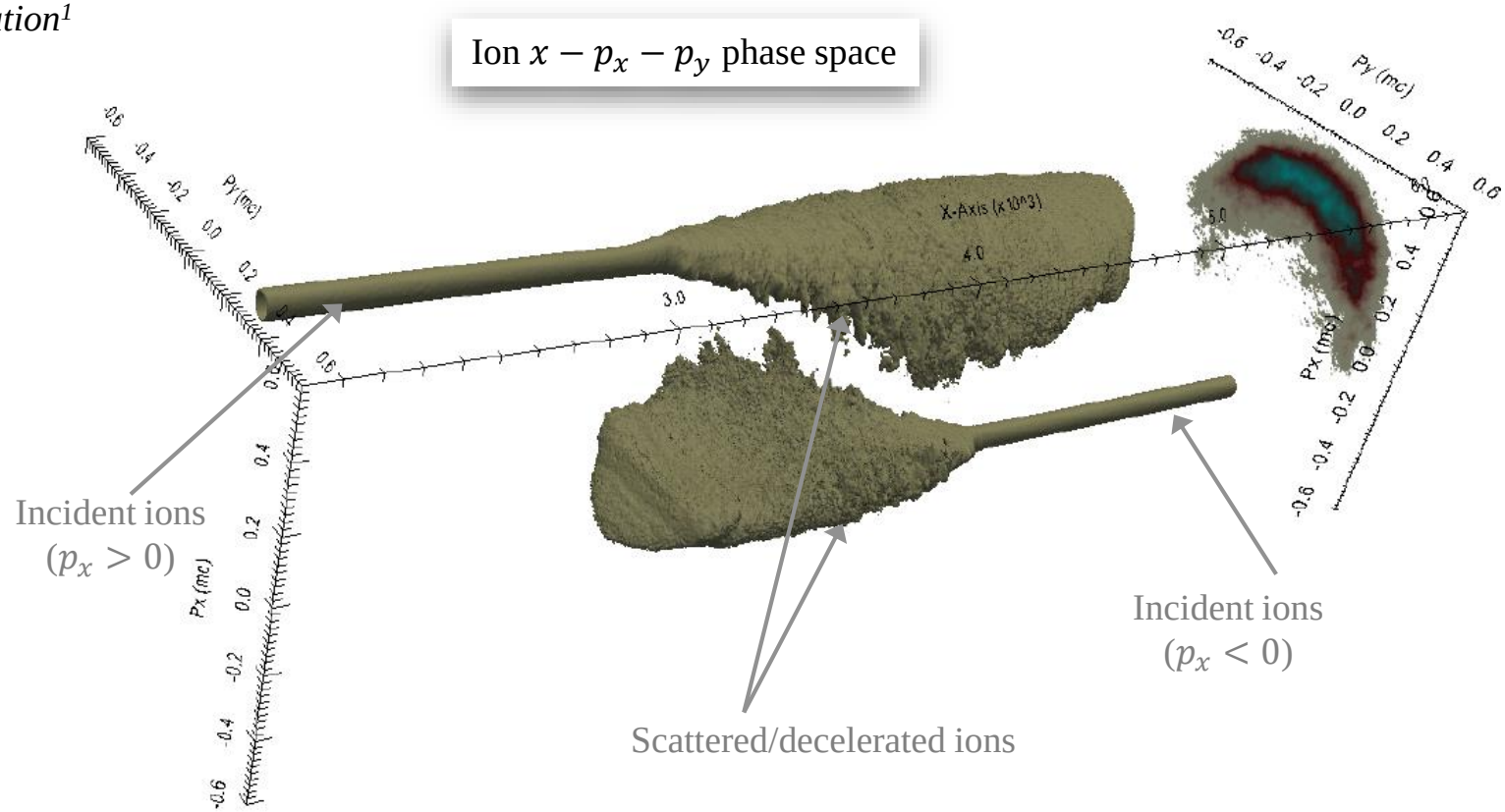

- Electron instabilities first develop and saturate, leaving the electrons mostly isotropized.
- The ion-ion Weibel-filamentation instability then develops up to $\sigma \equiv \langle B^2 \rangle / 2\mu_0 m_i c^2 (\gamma_i - 1) \sim 0.1$ (through filament coalescence and secondary kink instabilities), causing ion scattering off magnetic fluctuations.
- Isotropized particles accumulate in the overlap region until hydrodynamic-like (Rankine-Hugoniot) jump conditions are satisfied.

[1]C. Ruyer, PhD thesis, Université Paris-Sud (2014)

The experimental investigation of Weibel-mediated plasma collisions is becoming accessible to high-power lasers

- High-power lasers have the unique capability of driving high-velocity ($v_i \sim 0.001 - 0.1c$), high-density ($n_e > 10^{18}$ cm^{-3}) electron-ion plasmas from their interaction with dense targets.
- The simplest scheme consists in making collide two laser-generated plasma flows.
- Two types of lasers can be used:
  - High-energy ($>$ 10 kJ), moderate-intensity (10^{14-15} Wcm^{-2}), long-pulse ($>$ 1 ns) lasers
    $\Rightarrow$ non-relativistic interaction ($T_e \sim$ keV) and relatively slow flows ($v_i \sim 0.001 - 0.01c$).
  - High-intensity ($> 10^{19}$ Wcm^{-2}), moderate-energy ($\sim$ 0.1−1 kJ), short-pulse ($\sim$ 1 ps) lasers
    $\Rightarrow$ relativistic interaction ($T_e \sim$ MeV) and relatively fast ion flows ($v_i \sim 0.1c$).

High-energy, long-pulse laser scheme[1,2]

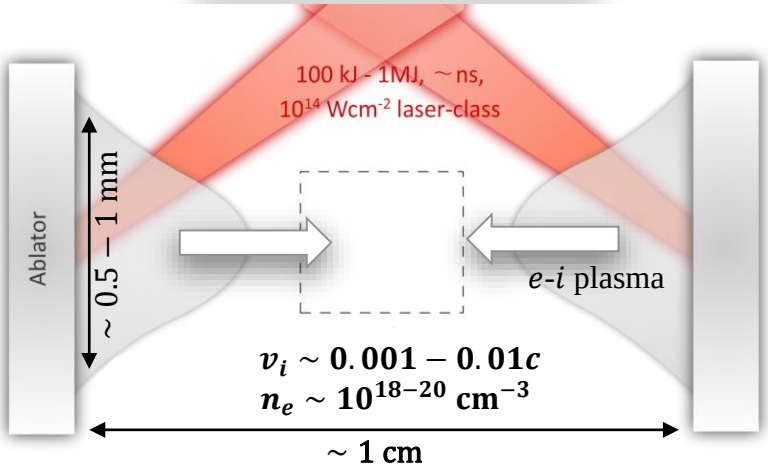

High-intensity, short-pulse laser scheme[3]

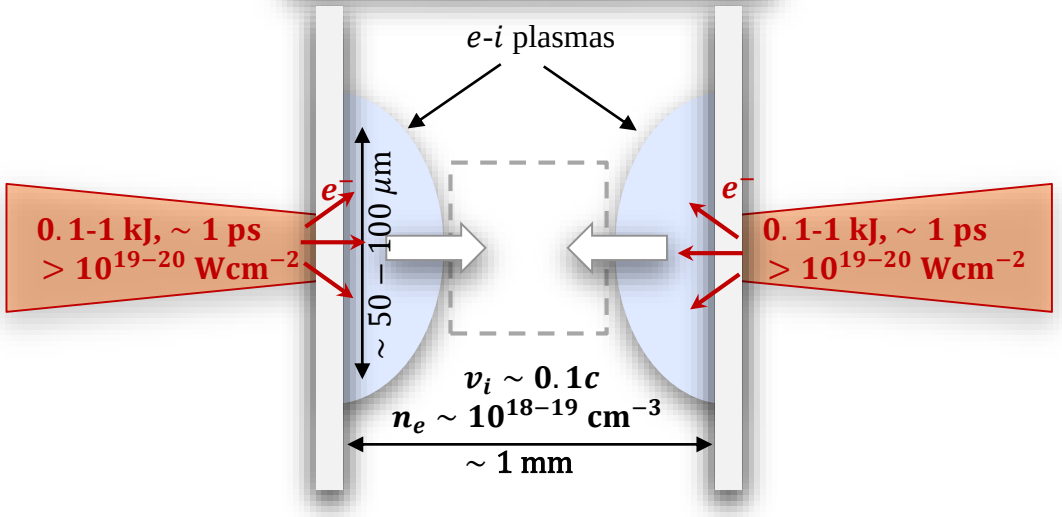

[1]W. Fox *et al.*, Phys. Rev. Lett. **111**, 225002 (2013)
[2]C.M. Huntington *et al.*, Nat. Phys. **11**, 173 (2015)

[3]S. P. Davis *et al.*, High Energy Density Phys. **9**, 231 (2013).

Multi-kJ-class lasers are required for shock generation

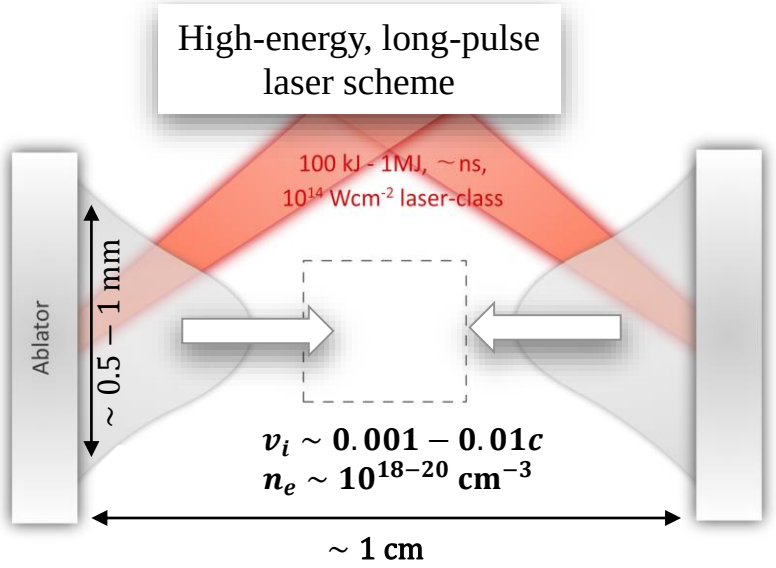

- Self-similar (1D) ablative flow: $n_{i,ss} \sim n_{ab} e^{-L_{int}/c_s t}$ where $n_{ab} \sim n_c \sim 10^{21}$ cm^{-3} (critical density) and $m_i n_{ab} c_s^3 \sim I_L \equiv 10^{15} I_{15}$ Wcm^{-2} ($Z = 1$ is assumed).
- Setting $L_{int} \sim 100 L_{100} c/\omega_{pi}$ and $t \sim \tau_L$ (laser duration), one has $\tau_L \sim \frac{100 c L_{100}}{\omega_{pi}\, c_s \ln n_{ab}/n_i}$.
- The condition $M_s \gg 1$ for Weibel-mediated shock implies $\ln \frac{n_{ab}}{n_e} \gg 1 \Rightarrow n_e \leq 0.01 n_{ab} \sim 10^{19}$ cm^{-3} .
- Assuming a laser spot radius $R_L \sim 10 R_{10} c/\omega_{pi}$ to accommodate enough ion filaments, the required laser energy to drive the shock-inducing collision can be estimated as

$$E_L[\text{kJ}] \geq 20 R_{10}^2 L_{100} n_{19}^{-3/2} I_{15}^{2/3}$$

- This estimate may be a very optimistic lower bound since, in practice, $R_L \ll L_{int} \Rightarrow n_i \ll n_{i,ss}$.

Formation and early nonlinear evolution of Weibel ion filaments recently observed in plasma-collision experiments[1,2]

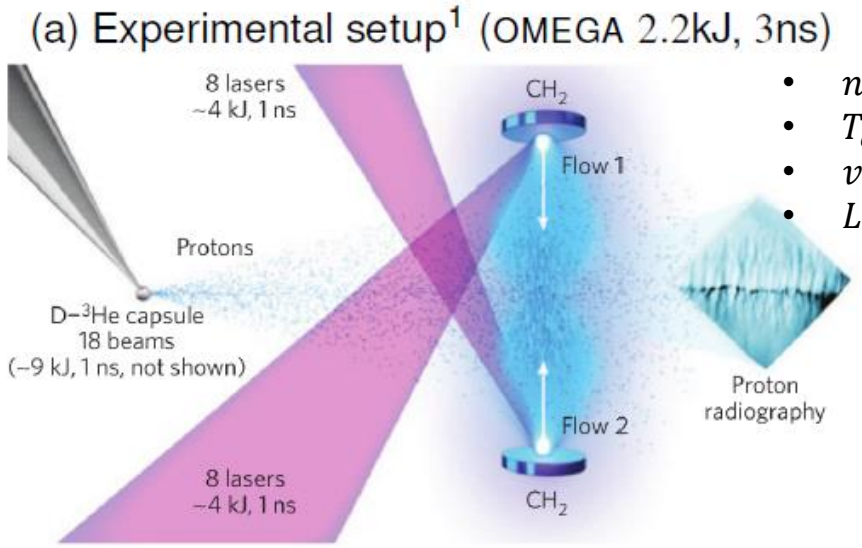

- $n_e \sim 5 \times 10^{18}$ cm^{-3}
- $T_e \sim 0.2$ keV
- $v_i \sim 2000$ kms^{-1} ($M_s \sim 20$)
- $L_{int} \sim 1$ cm $\sim 50 c/\omega_{pi}$

3D PIC (OSIRIS) simulation at $t = 1$ ns:
Isosurfaces of n_e(orange) and B (blue-red)

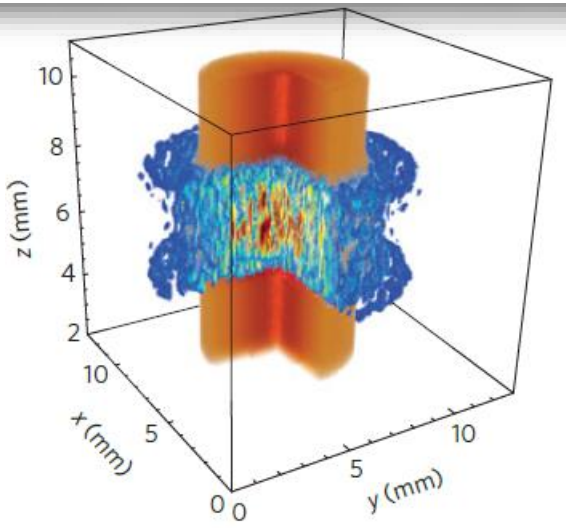

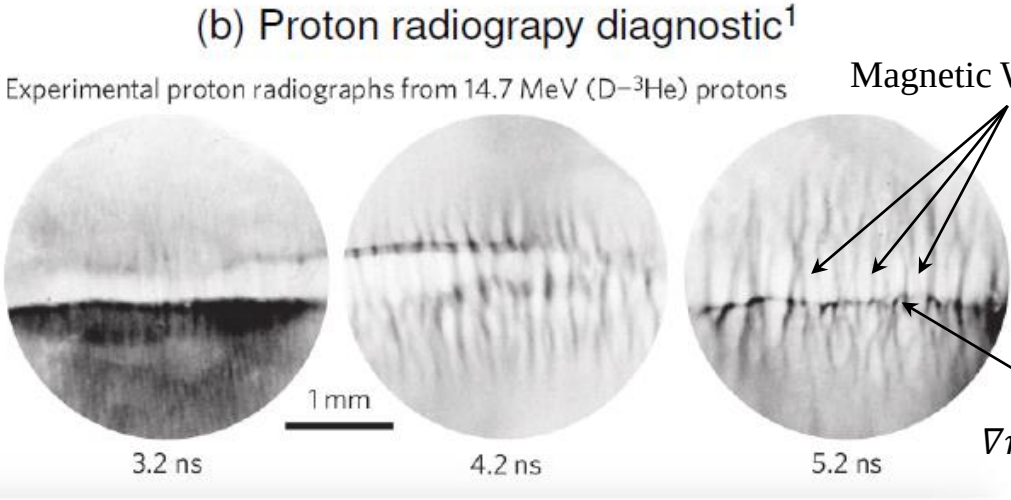

Magnetic Weibel filaments

Advected
$\nabla n \times \nabla T$ field

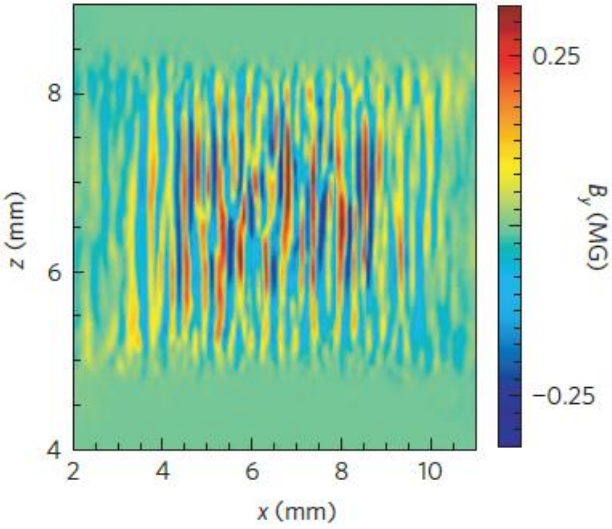

[1]C.M. Huntington *et al.*, Nat. Phys. **11**, 173 (2015)
[2]W. Fox et al., Phys. Rev. Lett. **111**, 225002 (2013)

Shock formation expected to be within the reach of the National Ignition Facility ($E_L \sim 1$ MJ)

Target design[1]

150 - 250 kJ per target
6 mm apart
Fe/Ni (0.1%) doped CD/CH foils

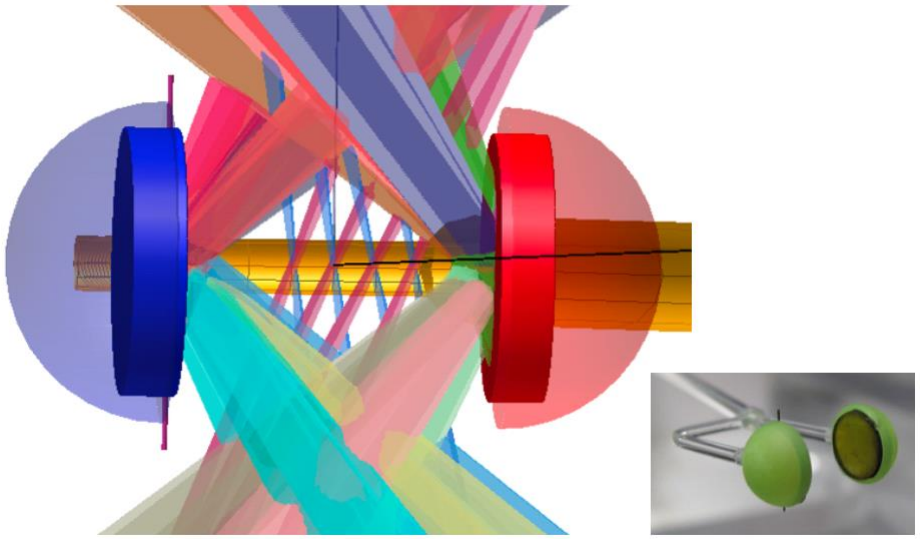

3D PIC (OSIRIS) simulation[1]

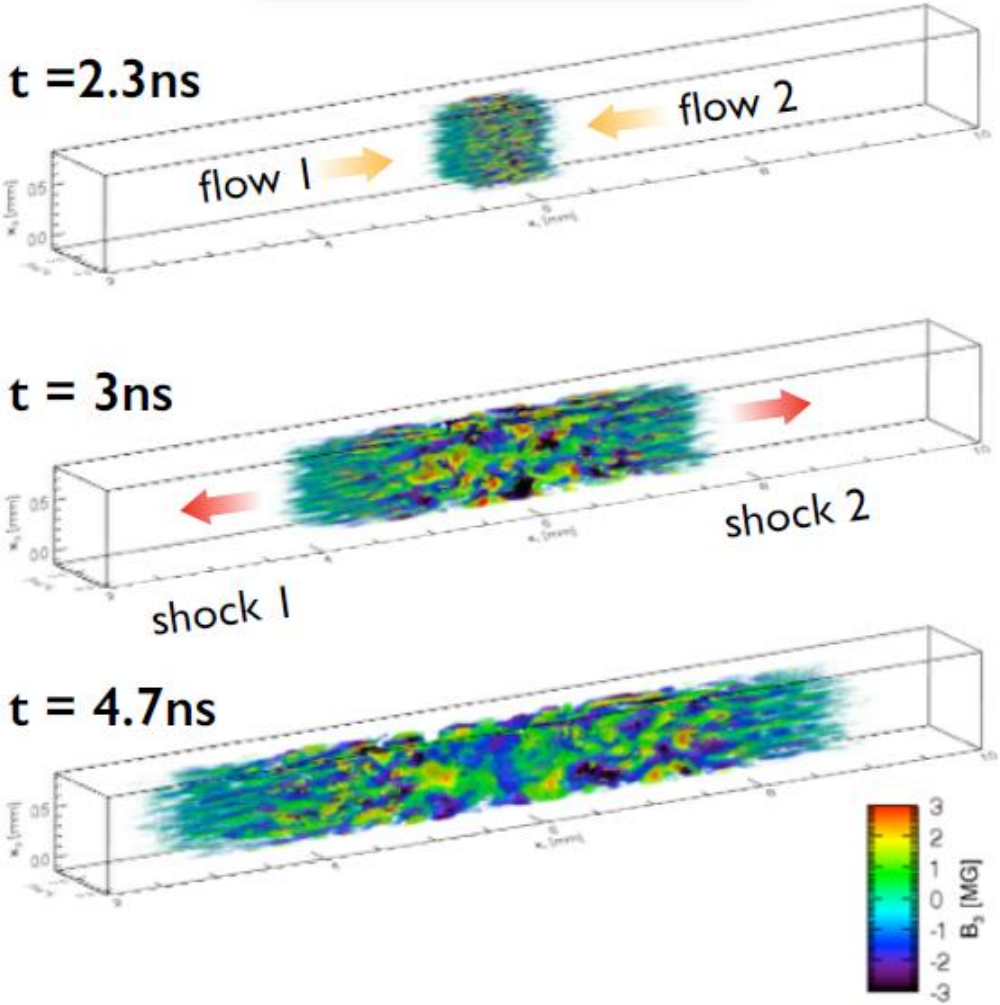

- Larger plasma densities ($\sim 2 \times 10^{20}$ cm^{-3}) are expected $\Rightarrow$ longer effective interaction length ($\sim 500c/\omega_{pi}$), yet instability development may be affected by collisions.
- PIC simulations performed with 'heavy' electrons ($m_{e,PIC} = 28m_e$) to reduce computing time.

[1]F. Fiuza, NIF/JLF Users Meeting 2015

A theoretical understanding of the shock formation dynamics is critical for extrapolating PIC results and designing experiments

- Even employing state-of-art supercomputers, numerical constraints posed by disparate e-i scales are such that PIC simulations of nonrelativistic shocks use artificially reduced ion-to-electron mass ratios (typically $m_i/m_e \leq 100$)[1-3].

⇒ **theoretical models are critically needed to extrapolate the simulation results to realistic conditions and thus help design laboratory experiments on high-energy lasers.**

- There exists a large discrepancy between proposed models/estimates for ion isotropization length (~ shock formation length):
  - $L_{iso} \sim 100 \frac{c}{\omega_{pi}} \propto m_i^{1/2}$ on the basis of low-m_i PIC simulations[1].
  - $L_{iso} \sim \left(\frac{m_i}{m_e}\right)^{\frac{3}{2}} \frac{c}{\omega_{pi}} \propto m_i^2$ from evaluating ion diffusion in stationary Weibel turbulence[4,5].
- In the following, we study the shock formation dynamics, and notably its ion-mass dependence, using large-scale particle-in-cell simulations and analytic modeling[6,7].

[1]A. Spitkovsky, Astrophys. J. **673**, L39 (2008)
[2]T. Kato and H.Takabe, Astrophys. J. **681**, L93 (2008)
[3]W. Fox *et al.*, Phys. Rev. Lett. **111**, 225002 (2013)
[4]C.M. Huntington *et al.*, Nat. Phys. **11**, 173 (2015)
[5]Y. Lyubarsky and D. Eichler, Astrophys. J. **647**, 1250 (2006)
[6]A. Achterberg *et al.*, A & A **475**, 19 (2007)
[7]C. Ruyer *et al.*, Phys. Plasmas **22**, 032102 (2015)
[8]C. Ruyer *et al.*, Phys. Rev. Lett. **117**, 065001 (2016)

The weakly-nonlinear ion Weibel instability in a symmetric two-beam system has been modeled using quasilinear kinetic theory[1,2]

- For a non-relativistic bi-Maxwellian distribution

$$f^{(0)} \propto \exp\left(-\frac{m(v_x - v_i)^2}{2T_{ix}} - \frac{mv_y^2}{2T_{iy}}\right)$$

- For $\xi_i = \Gamma/k_y v_{th,y} \ll 1$ and $f^{(0)} \equiv \langle f^{(0)}(\mathbf{r}, \mathbf{v}, t)\rangle_{\mathbf{r}}$ [1]

$$\partial_t f^{(0)} = \sum_{k_y} \frac{-i\omega_{pi}^2 |B_{k_y}|^2}{\mu_0 n_i m_i c^2 k_y^2} \left[-k_y v_x \partial_{v_y} + (\Gamma_{-k} + k_y v_y)\partial_{v_y}\right] \times \left[\frac{k_y v_x \partial_{v_y} + (\Gamma_k - k_y v_y)\partial_{v_y}}{\Gamma_k - k_y v_y}\right] f^{(0)}$$

  - The dispersion relation yields $k_y^2 + \Gamma_{k_y}^2 + \sum_{s\equiv i,e} \omega_{ps}^2 - \sum_{s\equiv i,e} \omega_{ps}^2 \frac{K_{sx}}{T_{sy}} [1 + \xi_s \mathcal{Z}(\xi_s)] = 0$
  - The quasilinear equations on the distribution moments read

$$\partial_t \int d\mathbf{v} v_x f^{(0)}/n_i \qquad = \partial_t v_s = -\sum_k Z_i^2 v_s / m_i T_{sy} \Re\left[1 + \xi_s \mathcal{Z}(\xi_s)\right] \partial_t |B_{k_y}|^2 / k_y^2$$

$$\partial_t \int d\mathbf{v} m_i v_y^2 f^{(0)}/n_i \quad = \partial_t T_{sy} = +\sum_k Z_i^2 / m_i (a_{ns} + 1) \Re\left[1 + \xi_s \mathcal{Z}(\xi_s)\right] \partial_t |B_{k_y}|^2 / k_y^2$$

$$\partial_t \int d\mathbf{v} m_i v_x^2 f^{(0)}/n_i \quad = \partial_t K_{sx} = -\sum_k Z_i^2 / m_i \Re\left[2(a_{ns} + 1)(1 + \xi_s \mathcal{Z}(\xi_s)) - 1\right] \partial_t |B_{k_y}|^2 / k_y^2$$

[1] R.C. Davidson *et al.*, Phys. Fluids **15**, 317 (1972)
[2] C. Ruyer et al., Phys. Plasmas **22**, 032102 (2015)

Approximate solutions can be found in the case of highly anisotropic ions and isotropic electrons[1]

- The ion anisotropy factor is $a_i = \frac{K_{ix}}{T_{iy}} - 1 \gg 1$
- In the weak-growth limit $\left|\sqrt{\frac{m_i}{2T_i}}\frac{\Gamma}{k_y}\right| \ll 1$, the maximum growth rate and associated wave vector simplify to

$$\Gamma_{sat} \approx \frac{2\omega_{pi}}{3}\sqrt{\frac{2T_{iy}a_i}{3\pi m_i c^2}} \text{ and } k_{sat} \approx \frac{\omega_{pi}}{\sqrt{3}c}\sqrt{a_i}$$

- The moment equations can then be approximated as

$$\partial_t v_i = -\alpha_i \frac{Z_i^2}{m_i}\frac{v_i}{T_{iy}}\partial_t S_p$$

$$\partial_t T_{iy} = \alpha_i \frac{Z_i^2}{T_{iy}}(a_i + 1)\partial_t S_p$$

$$\partial_t K_{ix} = -\frac{Z_i^2}{m_i}(2\alpha_i a_i + 2\alpha_i - 1)\partial_t S_p$$

where we have defined $S_p = e^2 \sum_{k_y} B_k^2/k_y^2$ and $\alpha_i \equiv 1 + \xi_{sat}Z(\xi_{sat}) \approx 0.5$.

- Noting that $\partial_t K_{ix}/\partial_t T_{iy} \approx -2$ to leading order in $1/a_i$, the previous system can be solved as

$$T_{iy}(t) = \sqrt{T_{iy}^2(0) + 2\alpha_i \frac{Z_i^2}{m_i} K_i(0)\,[S_p(t) - S_p(0)]}$$

$$a_i(t) = \frac{K_{iy}(0)}{\sqrt{T_{iy}^2(0) + 2\alpha_i \frac{Z_i^2}{m_i} K_i(0)[S_p(t) - S_p(0)]}} - 2$$

[1]C. Ruyer et al., Phys. Plasmas **22**, 032102 (2015)

A simple closure relation is provided by a filament coalescence argument

Periodic 3D PIC simulation with $v_i = \pm 0.2c, T_{e,i}/m_e c^2 = 0.01\,, m_i/m_e = 100$

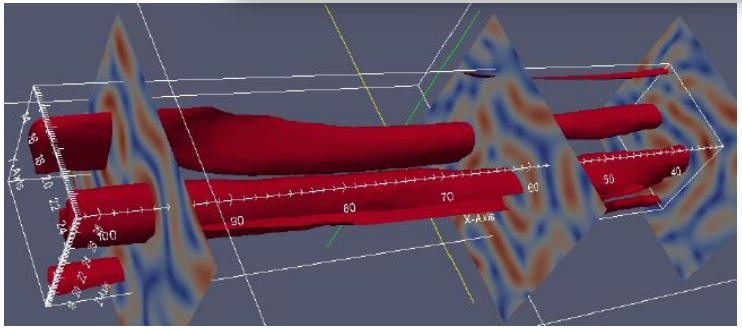

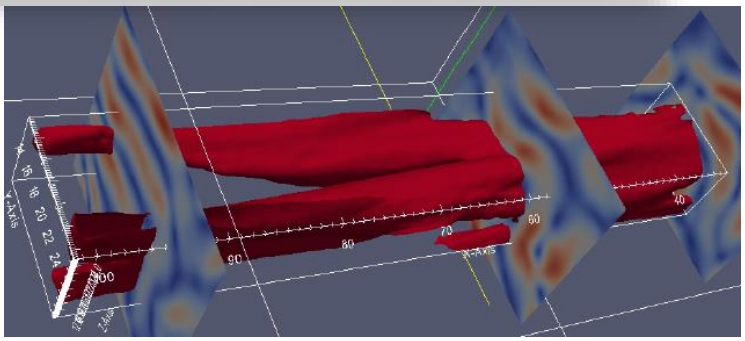

- The equation of motion applied to the distance between two filaments, d, gives

$$\ddot{d} \approx -\frac{j_x}{m_i n_i}\langle B_z\rangle \approx -\frac{Z_i e\kappa v_i}{m_i}\langle B_z\rangle \Rightarrow \Delta\dot{d}^2 \approx \frac{2Z_i e\kappa v_i}{m_i}\Delta\langle A_x\rangle(t)$$

  where $\kappa \approx \frac{2ck_{sat}}{\pi\omega_p}$ is the **electron screening factor**.

- Approximating $e\langle A_x\rangle \approx S_p^{1/2}$ and $|\dot{\lambda}_{sat}| \approx |\dot{d}|$, one can find

$$\dot{\lambda}^2_{sat} \approx \frac{\omega_{pi} v_0}{2\pi m_i\, \omega_{pe}} \int_{S_p(t^*)}^{S_p(t)} \frac{du}{\sqrt{u}} \left(\frac{m_i v_0}{\sqrt{2\alpha_i Z_i^2 u}}\right)^{1/2}$$

  where t^* denotes the start time of the nonlinear Weibel stage.

- There follows $\lambda_{sat} \approx \lambda^* \left(1 + \frac{\Delta t^2}{\tau_0^2}\right)$, where λ^* is the initial (saturated) wave-number, $\Delta t = t - t^*$, and $\tau_0 = \frac{2}{v_0}\left(\frac{4m_i}{Z_i m_e}\right)^{1/4}\sqrt{\frac{\lambda_* c}{\omega_{pi}}}$ is the typical **coalescence time** (note its $m_i^{3/4}/m_e^{1/4}$ scaling).

The obtained expressions of the time-dependent ion and spectral parameters are consistent with periodic PIC simulations[1]

- Introducing $G(t) = 1 + \Delta t^2/\tau_0^2$, one obtains:

$$\lambda_{sat}(t) \approx \lambda_* G(t)$$

$$S_p(t) \approx \frac{m_i^2 v_0^2}{2\alpha_i Z_i^2} \frac{G(t)^4}{a_i(t_*)+2G(t)^2}$$

$$a_i(t) \approx \left(\frac{2k_* c}{\omega_{pi}}\right)^2 G(t)^{-2}$$

$$T_{iy} \approx m_i v_0^2 \frac{G(t)^2}{a_i(t_*)+G(t)^2}$$

- We estimate the wavenumber at the beginning of the nonlinear phase, k_*, from Davidson's trapping model[2]:

$$S_p^{1/2}(t_*) \sim m_i \Gamma_{sat}^2 / Z_i^2 v_0 {k_*}^2$$

- These formulas capture fairly well the results of 2D and 3D PIC simulations in periodic geometry.

Periodic 2D PIC simulation with $v_i = \pm 0.2c$, $T_{e,i}/m_e c^2 = 0.01$, $m_i/m_e = 100$

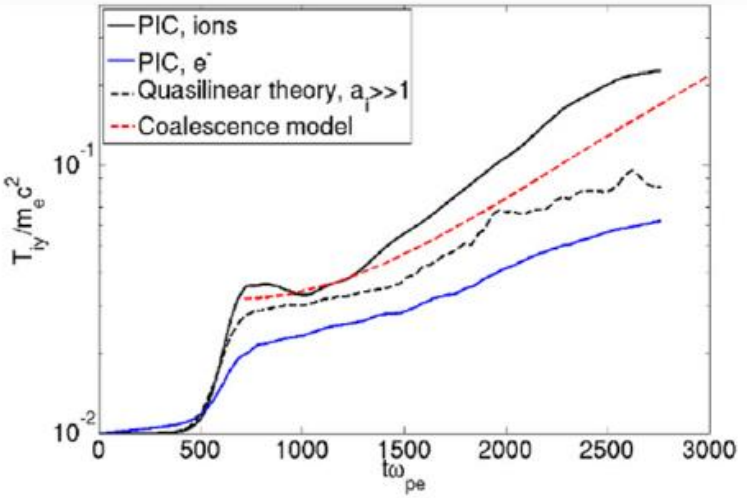

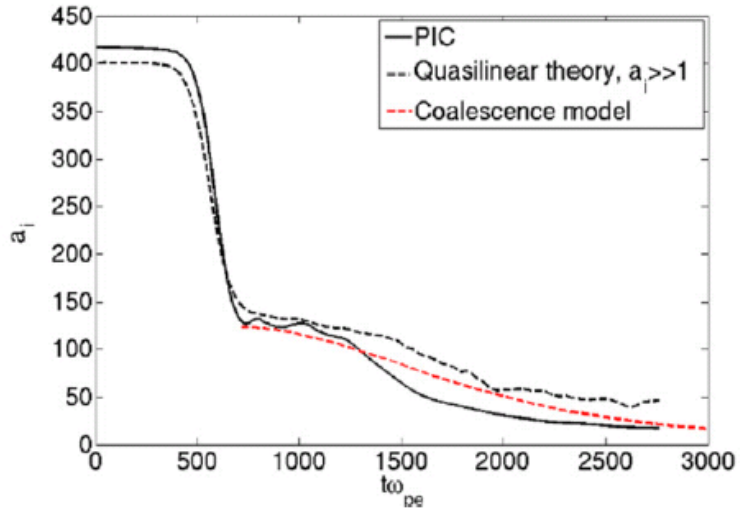

[1]C. Ruyer, L. Gremillet *et al.*, Phys. Plasmas **22**, 032102 (2015)
[2]R.C. Davidson *et al.*, Phys. Fluids **15**, 317 (1972)

Our theoretical model agrees with the experimentally measured filamentation dynamics[1,2]

- Time evolution of the filament spacing ($\lambda_{sat}/2$) as inferred from radiography measurements (green circles) and simulation (black triangles) of Refs.[1,2]. Blue solid line: QL model assuming $v_i \approx 1.9 \times 10^6 \mathrm{ms}^{-1}$, $n_e \approx 10^{19}$ cm^{-3} and initial wavenumber 130 μm $\leq \lambda^* \leq$ 190 μm. Red line: QL model with $m_e \times 28$ (as in the PIC simulation).

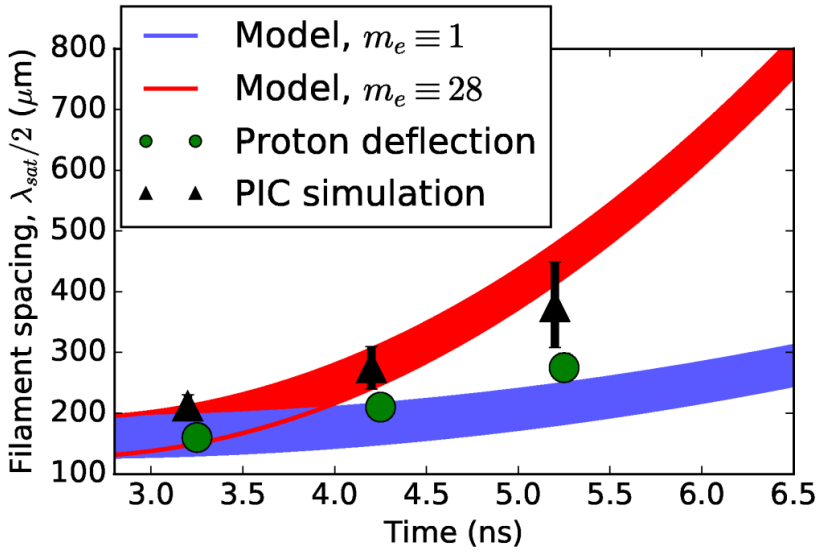

[1]C.M. Huntington *et al.*, Nat. Phys. 11, **173** (2015)
[2]H.S. Park *et al.*, Phys. Plasmas **22**, 056311 (2015)

- Instability still at its **early nonlinear stage** since $t - t^* < \tau_0 \approx 5$ ns (the interaction can be assumed symmetric).
- Good agreement found between the data and the theory, which reproduces the relatively weak variation of λ_{sat} over the observation time.
- Because of too heavy electrons ($m_e \times 28$), the PIC simulation overestimates the net current inside the filaments, thus **accelerating the coalescence process** by a factor $m_e^{1/4} \approx 2.3$. This behavior can be reproduced by our model by using the same artificially increased electron mass.

$\Rightarrow$ **Simulations with nonphysical m_i/m_e should be regarded with caution**, as the shock forms late in the instability's evolution ($t - t^* \gg \tau_0$), when important electron screening effects are expected.

To investigate the ion-mass dependence of the strongly-nonlinear shock formation phase, large-scale PIC simulations have been performed

- **2-D PIC simulation parameters (code CALDER[1])**
  - Symmetric plasma collision with flow velocities $v_i = \pm 0.4c$
  - $T_e = T_i = 5$ keV
  - Ion mass $m_i/m_e \in (25,100,400) \Rightarrow$ Mach number $M_s \in (30,60,120)$.
  - Simulation domain up to $L_x \times L_y = 16000 \times 800 \left(c/\omega_{pe}\right)^2$ with mesh sizes $\Delta x = \Delta y = 0.25c/\omega_{pe}$
  - Continuous particle injections through left & right boundaries.
  - 10 particles/cell/species initially $\Rightarrow$ final total number of particles $> 10^{10}$ for $m_i/m_e = 400$.
  - Binary collisions switched on (with boosted $\ln \Lambda = 10^5$) in upstream regions in order to damp spurious oscillations caused by particle injection.
  - Simulations run on up to 8000 cores.

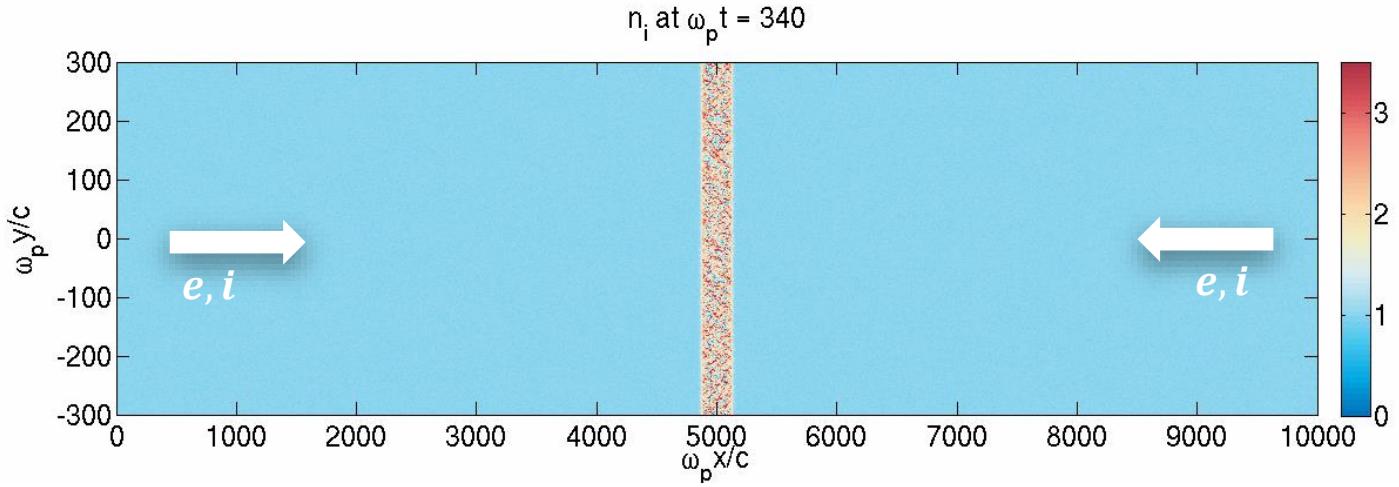

[1]E. Lefebvre *et al.*, Nucl. Fusion **43**, 629 (2003)

For $m_i/m_e = 25$, the shock forms at $t_{sh} \sim 1300\omega_{pe}^{-1} \sim 260\omega_{pi}^{-1}$

Total ion density

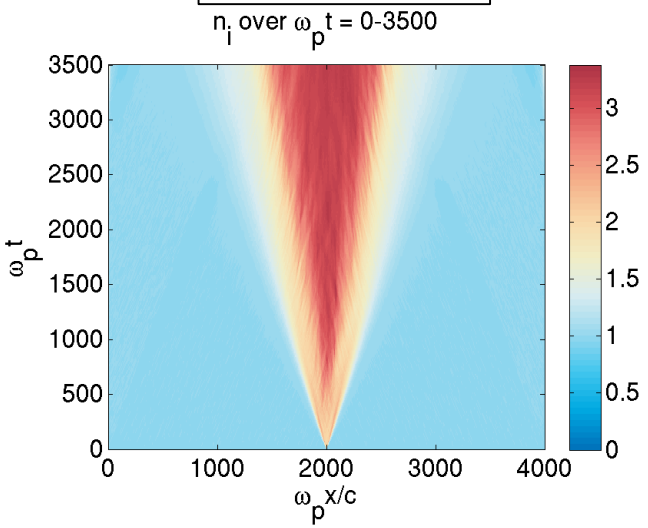

Anisotropy of the $v_x > 0$ injected ions

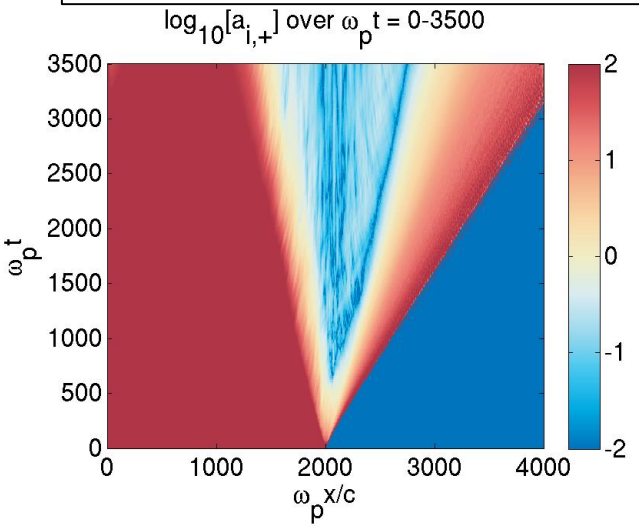

$\langle n_i \rangle$ at domain center

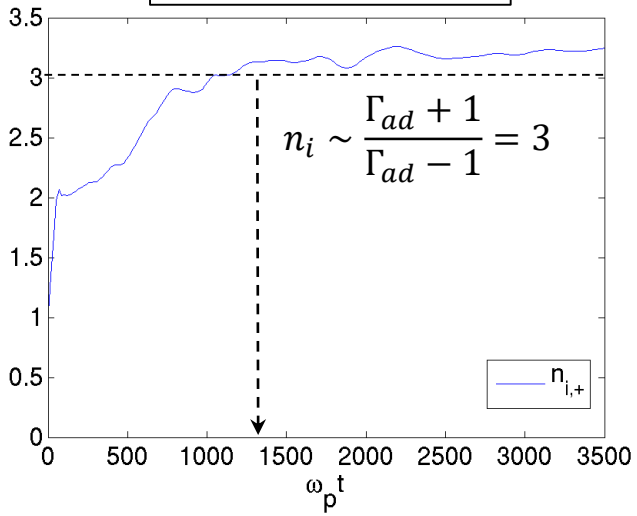

$\langle |a_{i+}| \rangle$ at domain center

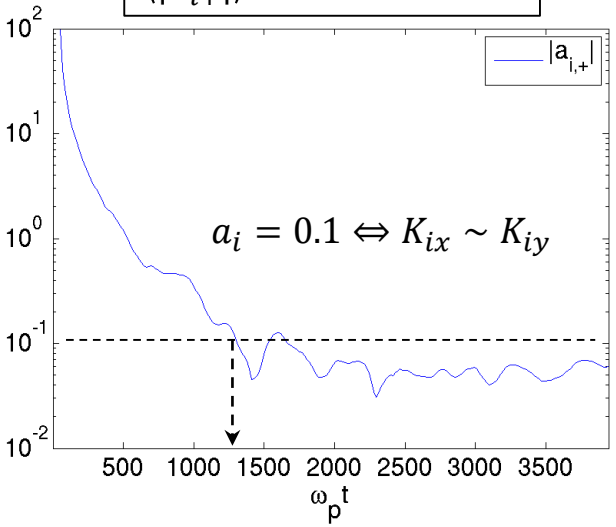

- The ion anisotropy factor is defined as
$$a_i = K_{ix}/K_{iy} - 1$$
where $K_{ix/y}$ is the ion momentum flux along the x/y axis.
- The shock formation time, t_{sh}, is close to the ion isotropization time $\simeq t_{a_i=0.1} \simeq 1300\ \omega_{pe}^{-1}$.
- Later on, the propagating shock fulfills the expected Rankine-Hugoniot jump conditions.

The shock forms at $t \sim 7000\omega_{pe}^{-1}$ ($\sim 700\omega_{pi}^{-1}$) for $m_i/m_e = 100$, yet is far from being formed at $t \sim 12000\omega_{pe}^{-1}$ for $m_i/m_e = 400$

Total ion density

Anisotropy of the $v_x > 0$ injected ions

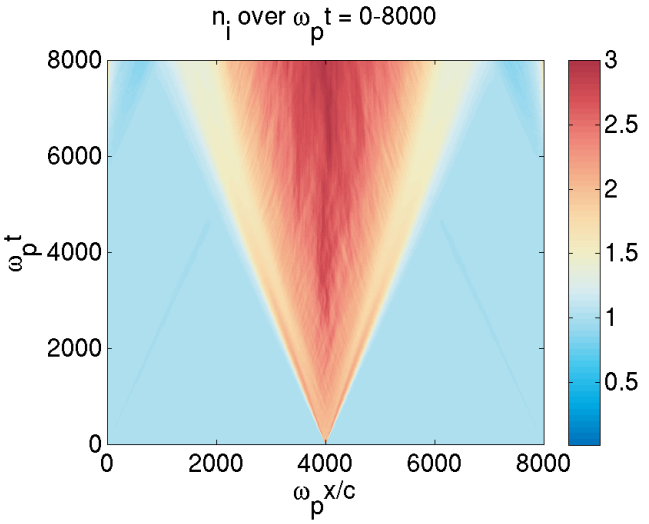

$m_i/m_e = 100$

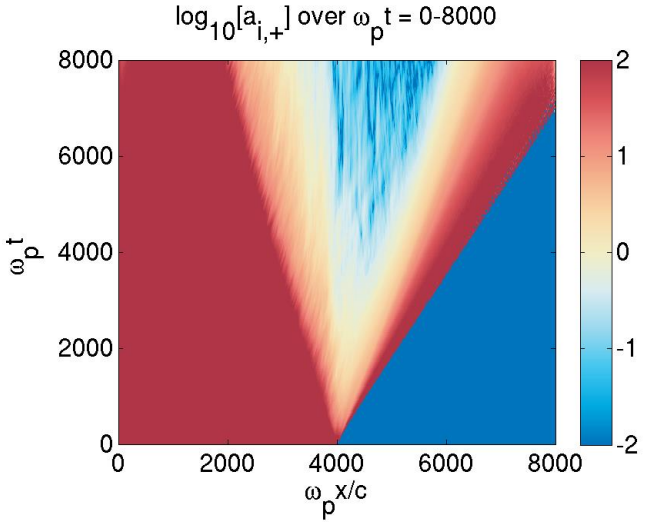

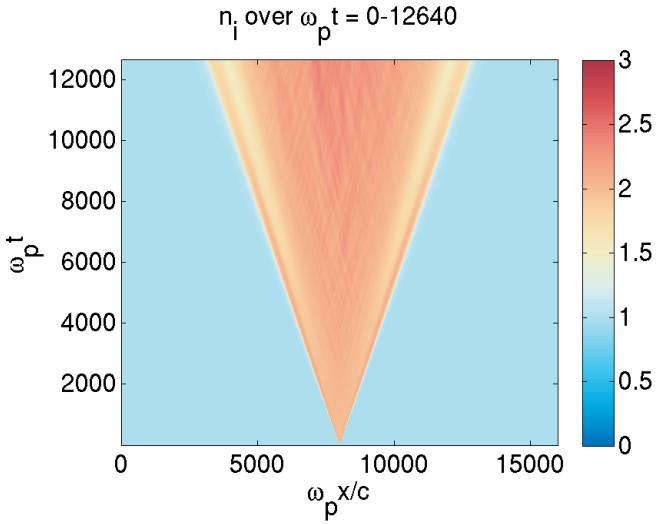

$m_i/m_e = 400$

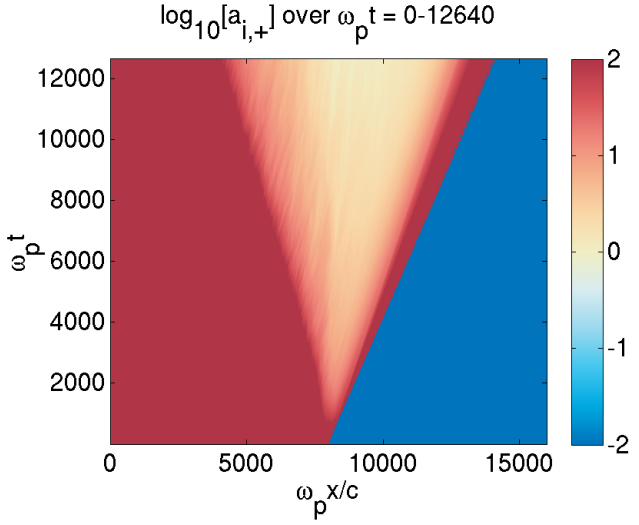

Case of $m_i/m_e = 400$: two filamentation stages can be identified in the overlap region

Density of the $v_x > 0$ injected ions

Density of the $v_x < 0$ injected ions

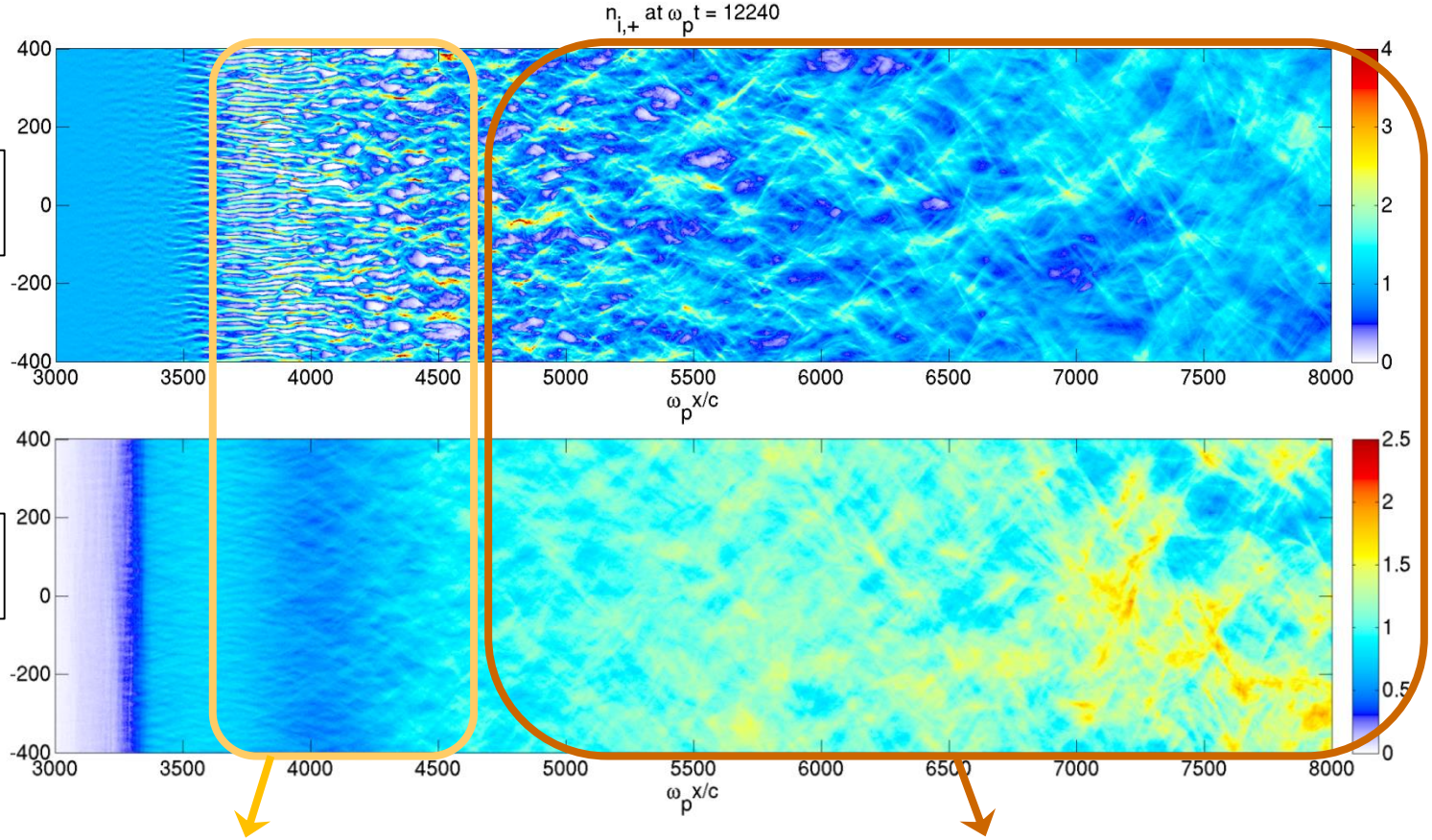

- Strong pinching ($\delta n/n \sim 1$) of the $v_x > 0$ ions
- Much hotter and weakly-modulated $v_x < 0$ ions
- Mainly transverse, electron-scale filaments ($k_y \sim 0.3\omega_{pe}/c$)
- Relatively weak transverse heating ($T_i < T_e$)
- $E_y \simeq v_{ix,+}B_z$ in filaments $\Rightarrow$ "Weibel frame" moves at $v_{ix,+}$

- Weaker kink-like current modulations
- Increasingly isotropic magnetic spectrum
- Strongly heated incoming ions ($T_{i+} \gg T_e$)
- $|v_{ix,+}B_z| \gg |E_y|$ in filaments
- Longer stage for $m_i/m_e \gg 1$, which lasts until full shock formation

Evolution of the magnetic spectrum in the overlap region

$\mathrm{sgn}(B_z)[3 + \log_{10}(10^{-3}, |B_z|)]$

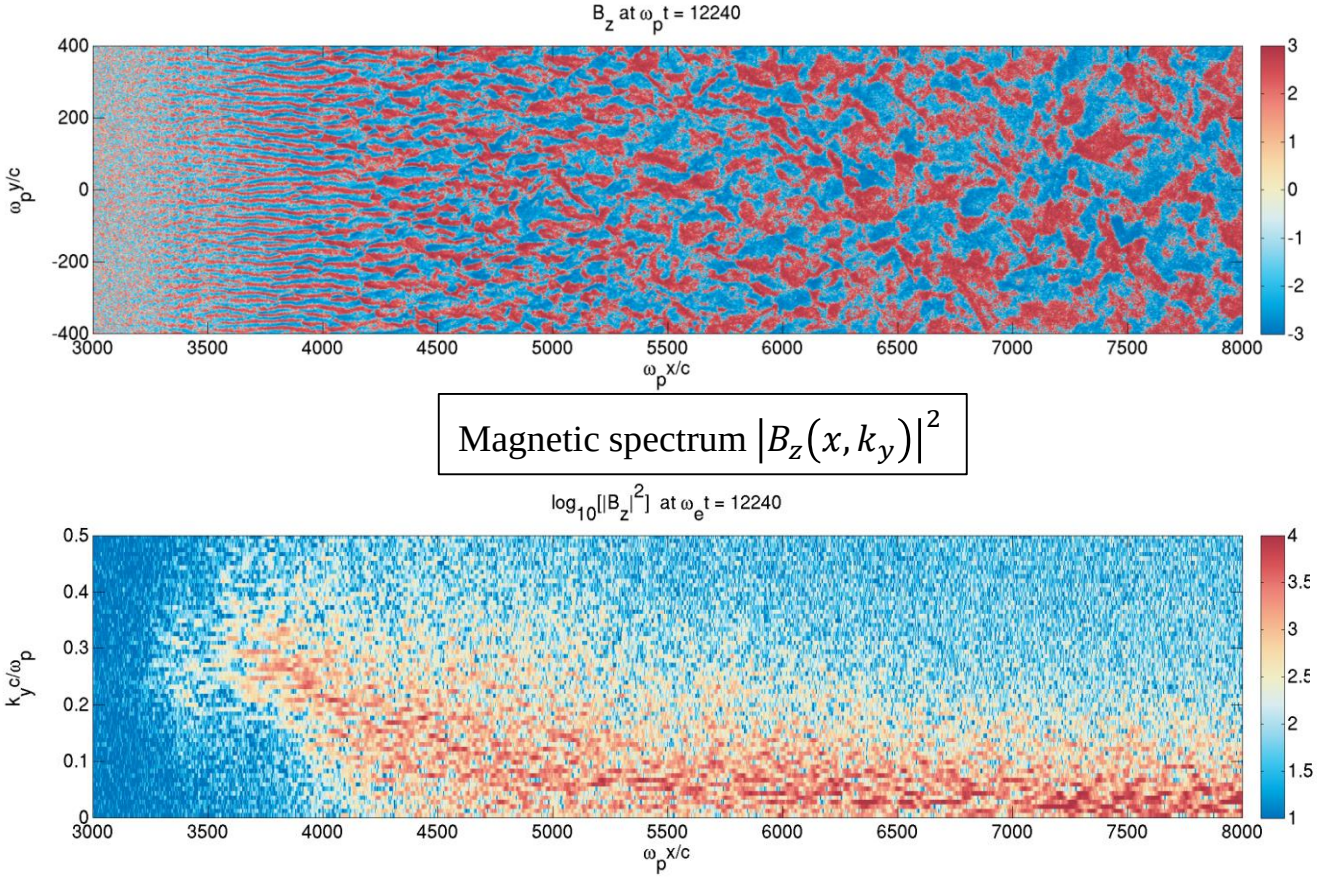

Magnetic spectrum $\left|B_z(x, k_y)\right|^2$

Magnetic energy $\langle B_z^2 \rangle_y$

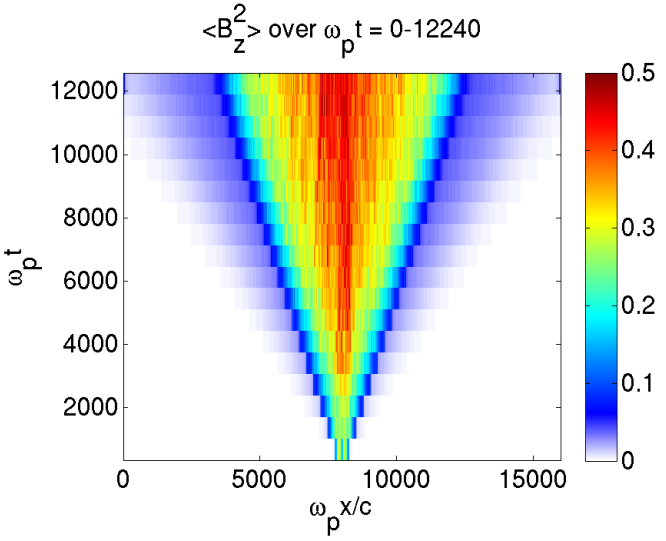

- Magnetic field energy saturates from $\omega_{pe}t \sim 2000 - 3000$ onwards (due to electron magnetization).
- Initially, $k_{y,max} \sim 0.3c/\omega_p$, similar to the value obtained for $m_i = 100$.
- $E_{x,y}^2$ energies negligible with respect to B_z^2 energy beyond $x \sim 4500c/\omega_{pe}$.

Magnetic spectra at different depths into overlap region show increasingly isotropic turbulence

$$\mathrm{sgn}(B_z)[3 + \log_{10}(10^{-3}, |B_z|)]$$

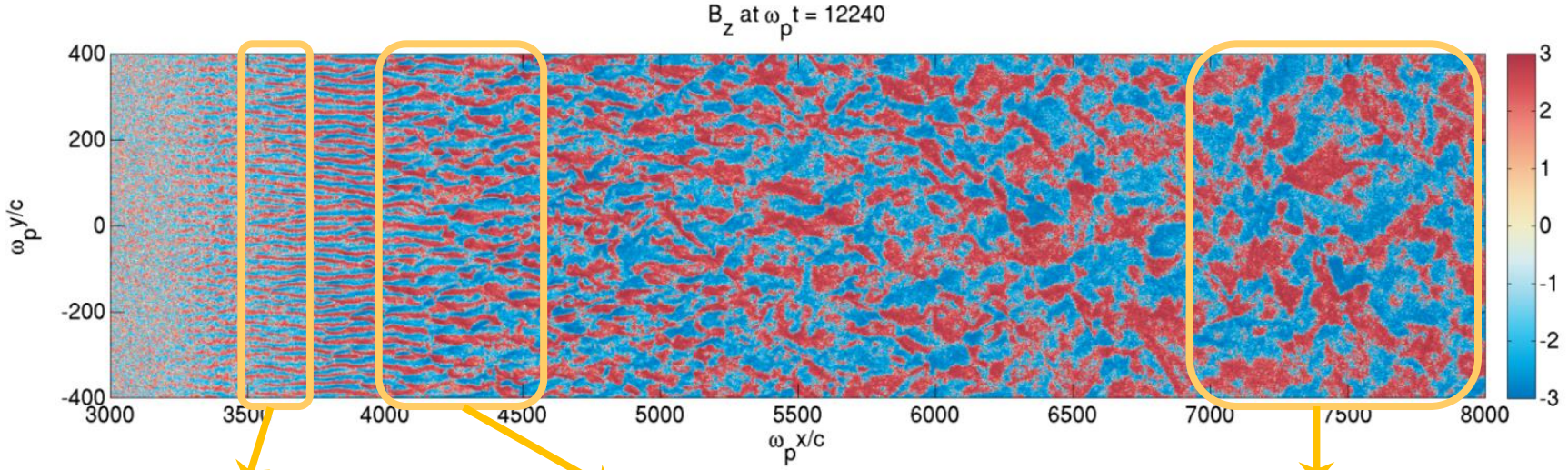

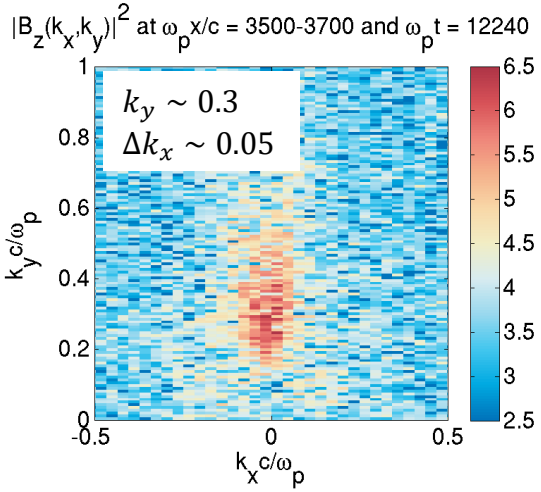

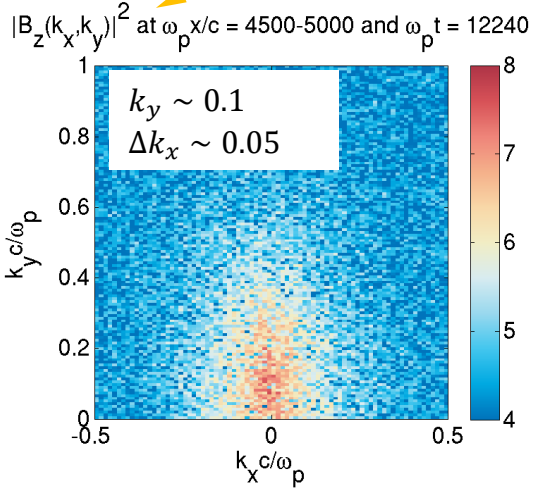

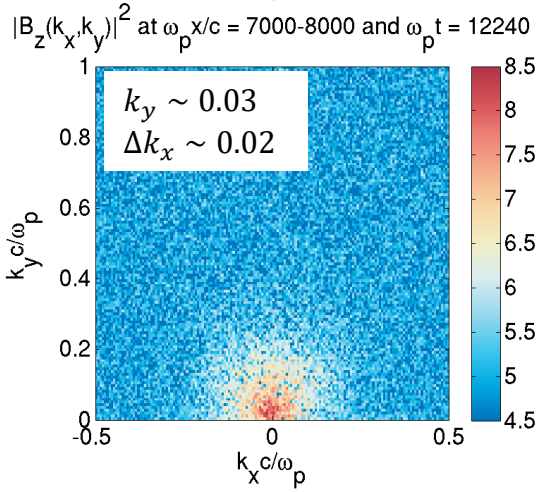

Dynamics of ion and electron heating

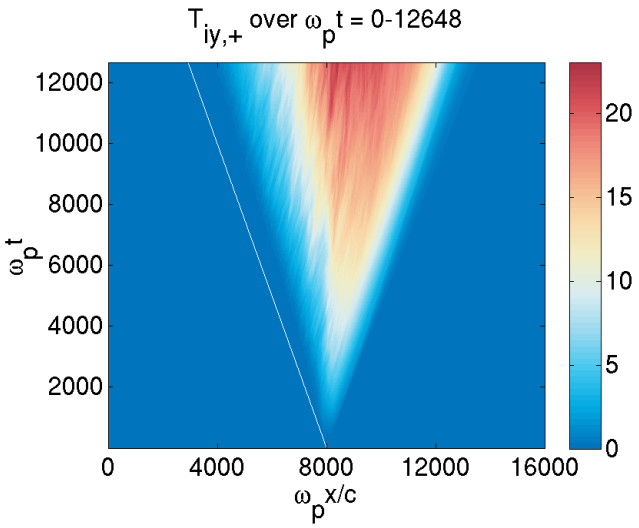

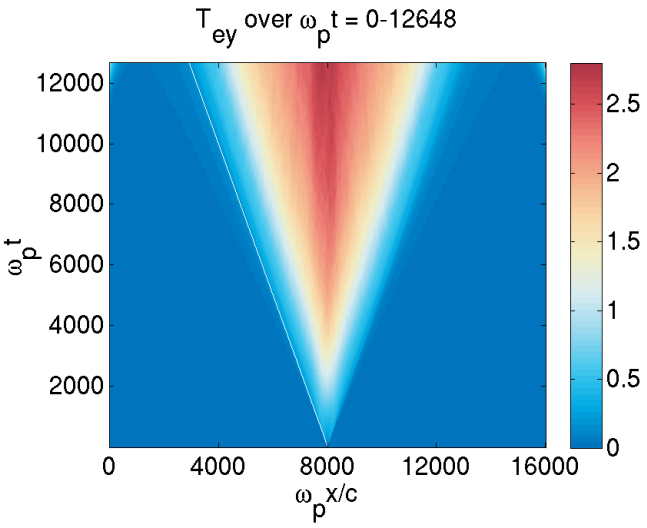

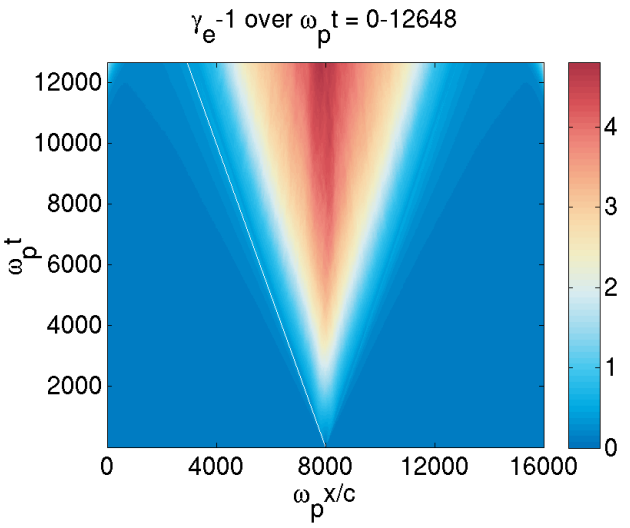

- Electrons essentially isotropized in the overlap region: $\gamma_e \sim 2T_e$.
- The electron skin depth and Larmor radius are both smaller than the pinched ion filaments
  $\Rightarrow$ electron magnetization effects expected.
- The incoming ions get much hotter than the electrons after a few filament mergers.
- T_{i+} and T_e essentially depend upon $\xi = x - x_c(t)$ where $x_c(t) = x_{mid} - v_0 t$.

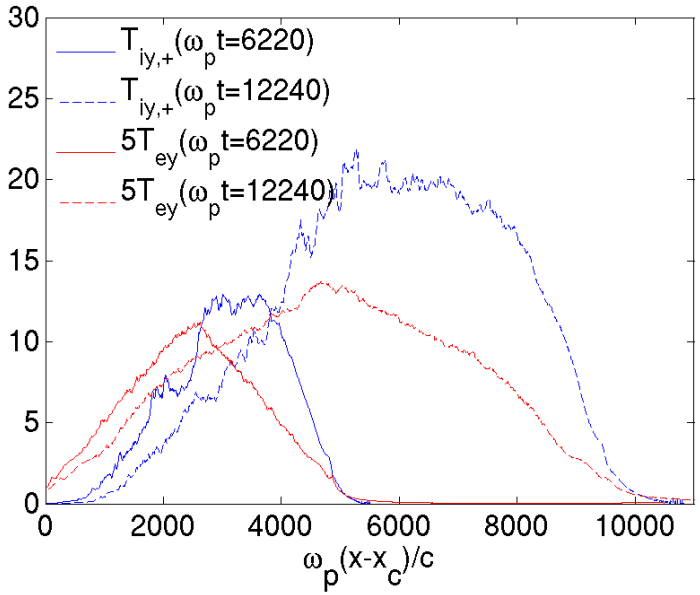

Analytical model of ion isotropization and shock formation[1]

- Asymmetric, nonlinear interaction considered here is poorly captured by previous QL model.
- Dominant filament wavelength under the conditions $T_e \ll T_c < T_h$:

$$\lambda_{sat} \simeq 4\pi \frac{c}{\omega_{pi}} \sqrt{\frac{2T_c}{m_i v_c^2}}$$

- Filament current density $j_x \simeq \kappa_e j_c$ with $j_c \simeq Z_i e n_c v_i$ and electron screening factor[2]

$$\kappa_e(t) \simeq 4c/\omega_{pe}\lambda_{sat}(t)$$

$\Rightarrow$ Magnetic field strength $B_z \simeq v_c\sqrt{\mu_0 Z_i m_e n_i}$, so that $T_c \simeq Z_i e^2 \langle A_x^2 \rangle / m_e$.

- From the estimate[3] $\Delta\left(m_i \dot{\lambda}_{sat}^2\right) \simeq \frac{j_x}{n}\Delta\sqrt{\langle A_x^2 \rangle}$, we get:

$$\partial_t \lambda_{sat} \simeq v_c \sqrt{\frac{Z_i m_e}{2\pi m_i} \ln\left(\frac{\lambda_{sat}}{\lambda_*}\right)}$$

where $\lambda_* \equiv \lambda(t_*)$ is the wavelength at the end time of the linear phase $t_*(x)$.

- Finally,

$$\lambda_{sat}(t,x) \simeq \lambda_* \exp\left[\mathrm{erfi}^{-1}\left(\frac{\Delta t}{\tau}\right)^2\right]$$

where $\Delta t = t - t_*(x)$ and $\tau = \frac{\pi\lambda_*}{v_c}\sqrt{\frac{2m_i}{Z_i m_e}}$

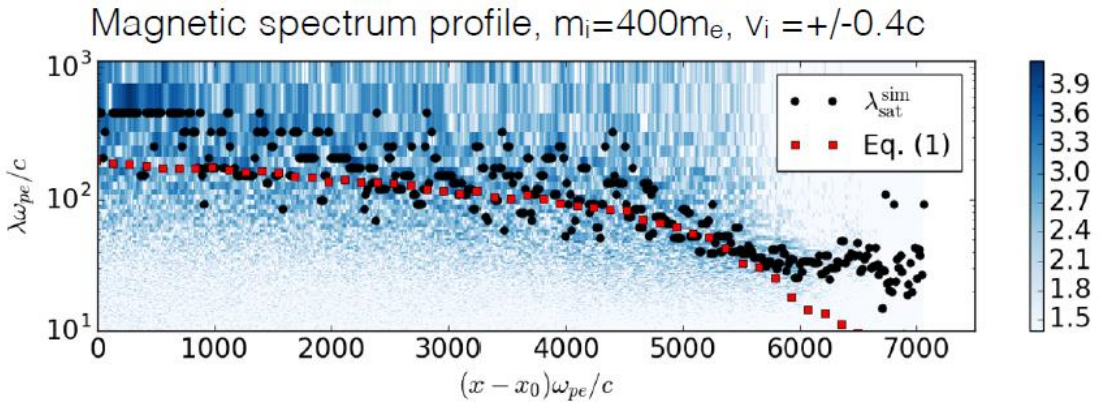

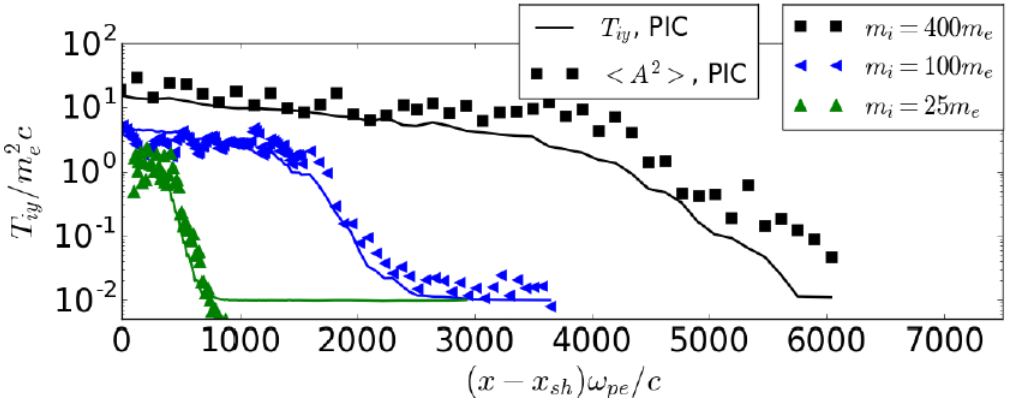

[1]C. Ruyer *et al.*, Phys. Rev. Lett. **117**, 065001 (2016)
[2]A. Achterberg *et al.*, A&A **475**, 19 (2007)
[3]C. Ruyer *et al.*, Phys. Plasmas **22**, 032102 (2015)

Our model fairly agrees with the simulation results

- Ion isotropization corresponds to
$$T_{cy}(t_{iso}) \simeq m_i v_c^2/2$$
- The magnetic wavelength is then
$$\lambda_{sat}(t_{iso}) \simeq \frac{4\pi c}{\omega_{pi}}$$

attained over a distance

$$L_{iso} \simeq \frac{40c}{\omega_{pi}} \mathrm{erfi}\left(\sqrt{\ln \frac{m_i}{Z_i m_e}}\right)$$
$$\simeq 35 \left(\frac{m_i}{Z_i m_e}\right)^{0.4} \frac{c}{\omega_{pi}}$$

- The obtained scaling $L_{iso} \propto m_i^{0.9}$ is stronger than the $m_i^{1/2}$ scaling proposed by Kato & Takabe[1], yet much less constraining than $L_{iso} \propto m_i^2$ predicted by evaluating ion diffusion in a static magnetic turbulence[2].
- The PIC results, however, suggest a somewhat stronger m_i scaling ($\propto m_i^{1.1}$).

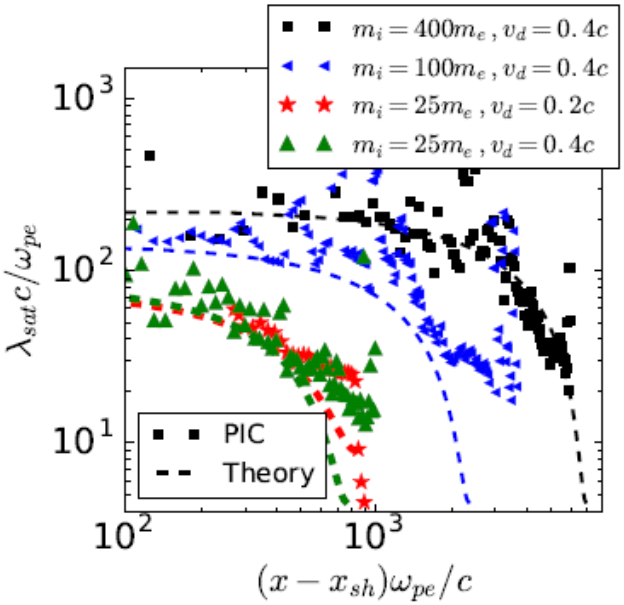

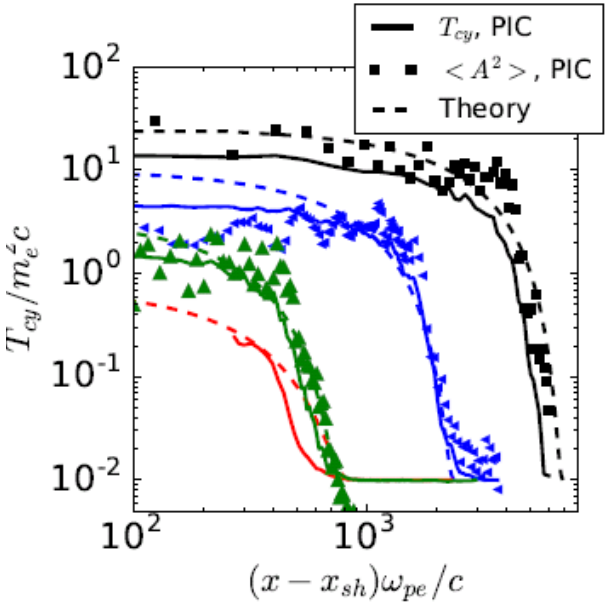

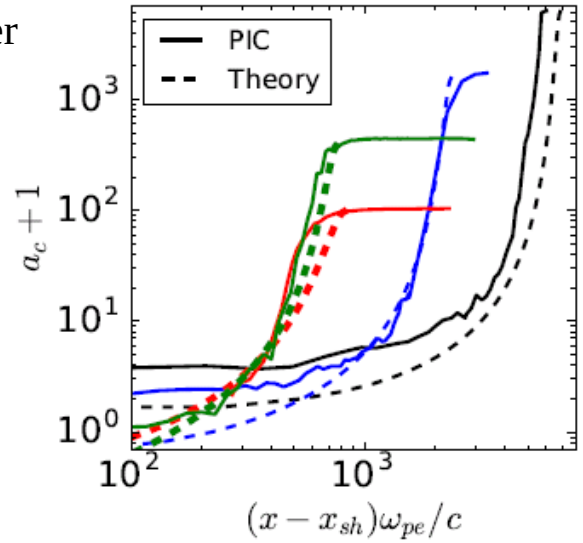

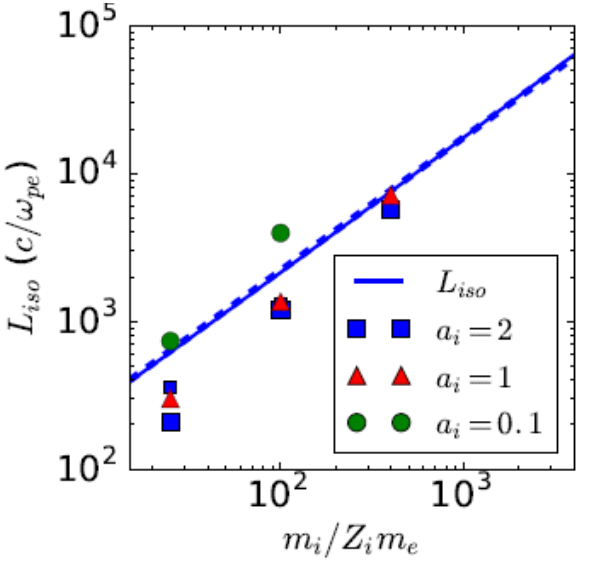

[1]T. Kato and H. Takabe, ApJ **681**, L93 (2008).
[2]Y. Lyubarsky and D. Eichler, ApJ **647**, 1250 (2006).

Conclusions

- High-power lasers enable experimental investigation of Weibel-instability-mediated plasma collisions.
- Ab initio PIC simulations allow self-consistent description of collisionless turbulent shocks, yet usually employ artificially low m_i/m_e to reduce computational load.
- Large-scale PIC simulations clarify the nonlinear interaction phase leading to shock formation.
- A simple analytical model, accounting for electron screening effects, correctly captures the simulation results up to the point of full ion isotropization, and can be used for designing laser experiments under conditions as yet inaccessible to PIC simulations.
- Our 2D results suggest that shock generation requires an interaction length $\geq 1000c/\omega_{pi}$, and hence a laser energy > 100 kJ per ablated target. The actual threshold energy being possibly significantly higher due to 3D geometry effects, this could explain the failure so far to achieve shock formation.

DE LA RECHERCHE À L'INDUSTRIE

Backup slides

Collisionless turbulent shocks may explain various high-energy astrophysical phenomena

- Collisionless turbulent shocks are held responsible for energetic particle and radiation generation in powerful space environments (supernovae remnants, gamma-ray bursts, pulsar wind nebulae…)[1]
- The Weibel-filamentation instability[2] seems a key player for shock formation in non/weakly-magnetized settings[3]:
  - develops in counter-streaming and/or anisotropic plasmas;
  - generates magnetic micro-turbulence acting as magnetic barrier and initiating shock transition;
  - provides scattering centers causing nonthermal particle acceleration and radiation emission.

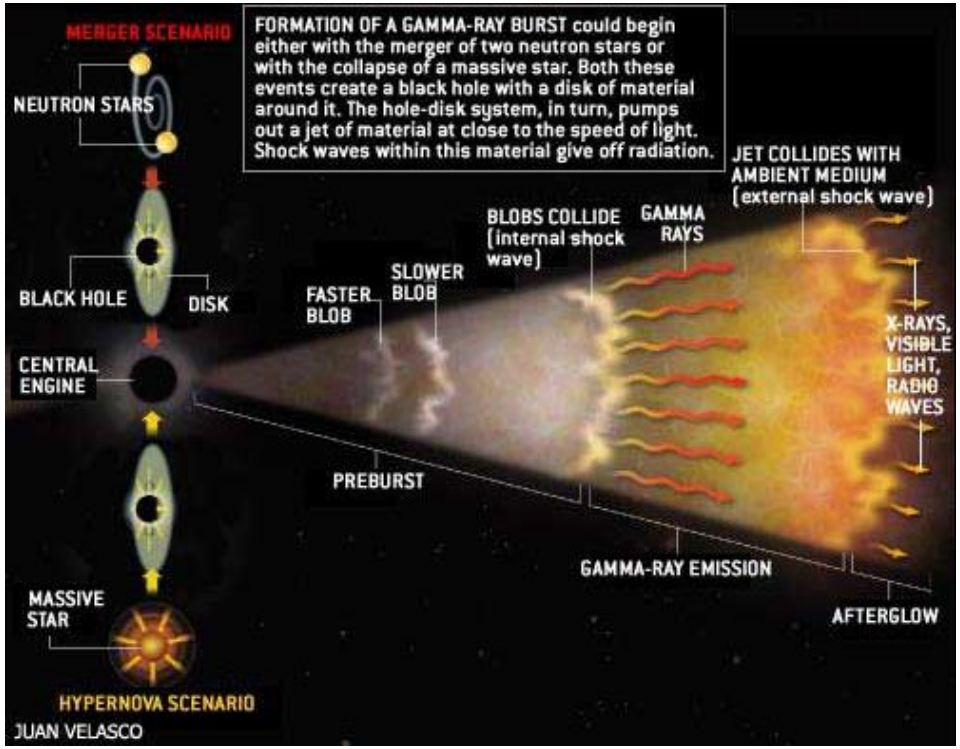

Principle of the Weibel-filamentation instability

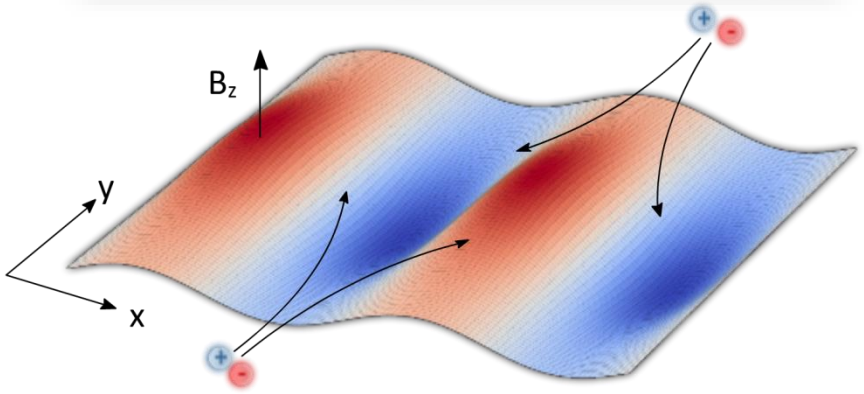

[1]T. Piran, RMP **76**, 1143 (2005); M. Lemoine *et al.*, ApJ **645**, L129 (2006).
[2]E. S. Weibel, PRL **2**, 83 (1959); M.V, Medvedev & A. Loeb, ApJ **526**, 697 (1999)
[3]A.Spitkovsky, APJ **682**, L5 (2008); M. Lemoine *et al*, MNRAS **417**, 1148 (2011)

Periodic PIC simulations support the obtained relations between the ion parameters and the magnetic power spectrum

- Noting that $\partial_t K_{ix}/\partial_t T_{iy} \approx -2$ to leading order in $1/a_i$, the previous system can be readily solved as

$$T_{iy}(t) = \sqrt{T_{iy}^2(0) + 2\alpha_i \frac{Z_i^2}{m_i} K_i\ (0)[S_p(t) - S_p(0)]}$$

$$v_i(t) = v_i(0)\exp\left[-\frac{2}{K_i(0)}\left(T_{iy}(t) - T_{iy}(0)\right)\right]$$

$$a_i(t) = \frac{K_{iy}(0)}{\sqrt{T_{iy}^2(0) + 2\alpha_i \frac{z_i^2}{m_i} K_i(0)[S_p(t) - S_p(0)]}} - 2$$

Periodic 2D PIC simulation with $v_i = \pm 0.2c$
$T_{e,i}/m_e c^2 = 0.01\ , m_i/m_e = 100$

Temporal evolution of $-\partial_t K_{ix}/\partial_t T_{iy}$

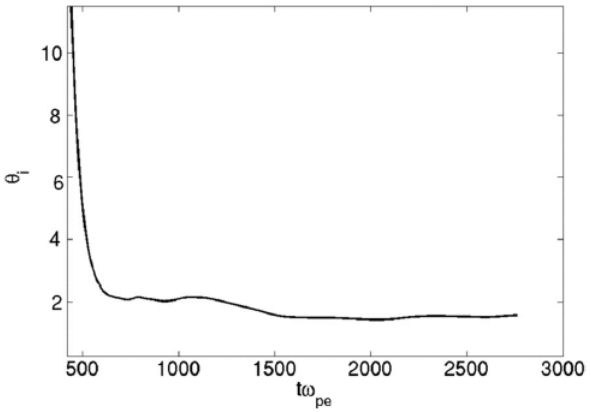

Mean ion x-velocity

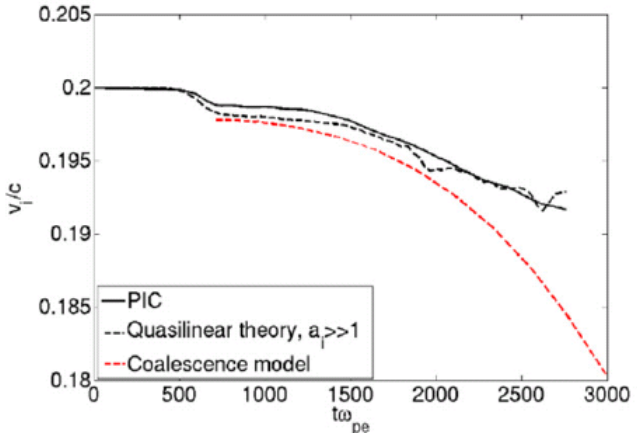

Ion anisotropy ratio

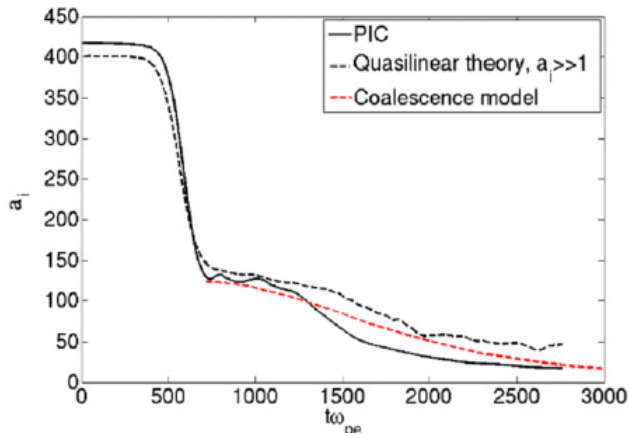

Transverse temperatures

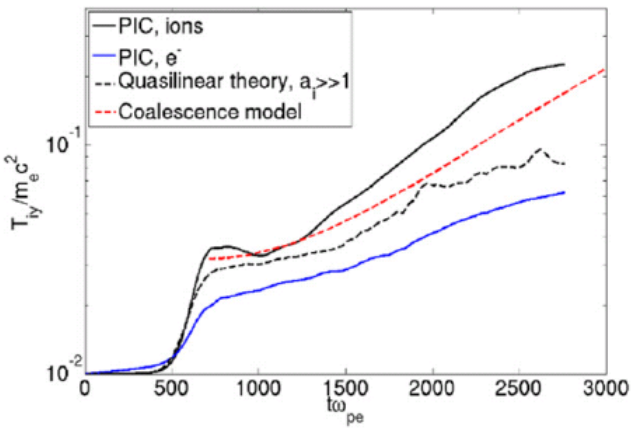

Approximate solutions can be found in the case of highly anisotropic ions and isotropic electrons[1]

- The ion anisotropy factor is $a_i = \frac{K_{ix}}{T_{iy}} - 1 \gg 1$
- In the weak-growth limit $\left|\sqrt{\frac{m_i}{2T_i}}\frac{\Gamma}{k_y}\right| \ll 1$, the maximum growth rate and associated wave vector simplify to

$$\Gamma_{sat} \approx \frac{2\omega_{pi}}{3}\sqrt{\frac{2T_{iy}a_i}{3\pi m_i c^2}} \text{ and } k_{sat} \approx \frac{\omega_{pi}}{\sqrt{3}c}\sqrt{a_i}$$

- The moment equations can then be approximated as

$$\partial_t v_i = -\alpha_i \frac{Z_i^2}{m_i}\frac{v_i}{T_{iy}}\partial_t S_p$$
$$\partial_t T_{iy} = \alpha_i \frac{Z_i^2}{T_{iy}}(a_i + 1)\partial_t S_p$$
$$\partial_t K_{ix} = -\frac{Z_i^2}{m_i}(2\alpha_i a_i + 2\alpha_i - 1)\partial_t S_p$$

where we have defined

$$S_p = e^2 \sum_{k_y} B_k^2/k_y^2$$
$$\alpha_i \equiv 1 + \xi_{sat} Z(\xi_{sat}) \approx 0.5.$$

$$v_i = \pm 0.2c, v_e = 0$$
$$T_{e,i} = 0.05 m_e c^2, \frac{m_i}{m_e} = 25$$

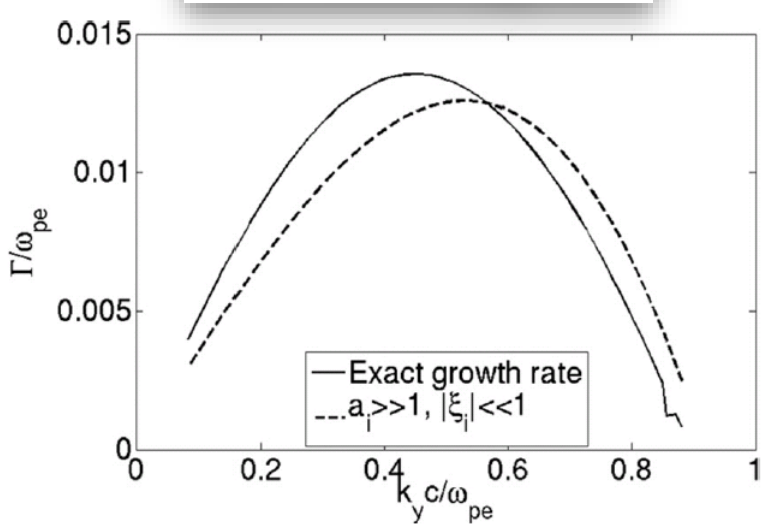

[1]C. Ruyer et al., Phys. Plasmas **22**, 032102 (2015)

Case $m_i/m_e = 400$: shock far from being formed by $t \sim 13000\omega_p^{-1}$ $(650\omega_{pi}^{-1})$

Total ion density

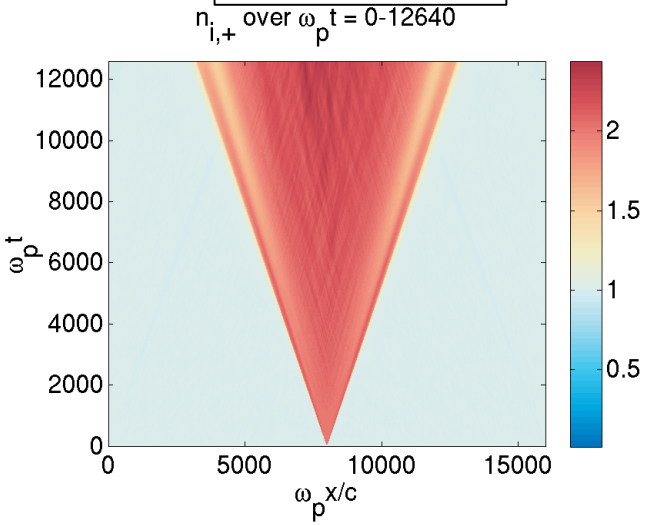

Anisotropy of the $+x$ injected ions

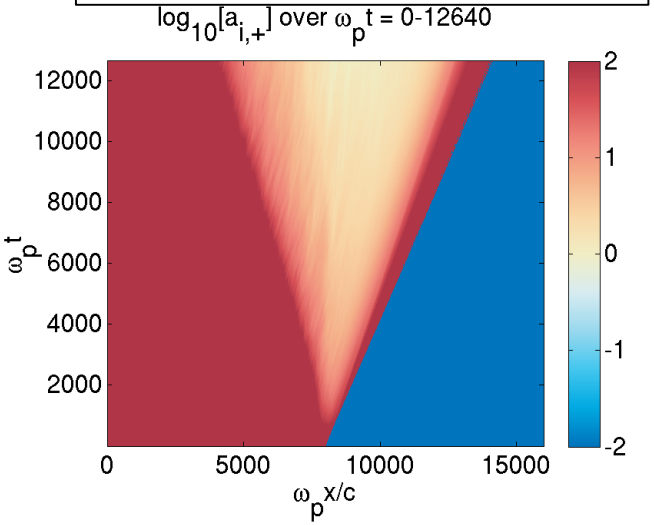

- Anisotropy at final simulation time: $a_i(t = 12600) \sim 1.3$
- Temperature at mid-plane rises linearly with time (while is expected to saturate at shock formation, see $m_i = 100$).
- Simulation domain too small to enable shock formation.

$\langle n_i \rangle$ over $x = L_x/2 \pm 80$

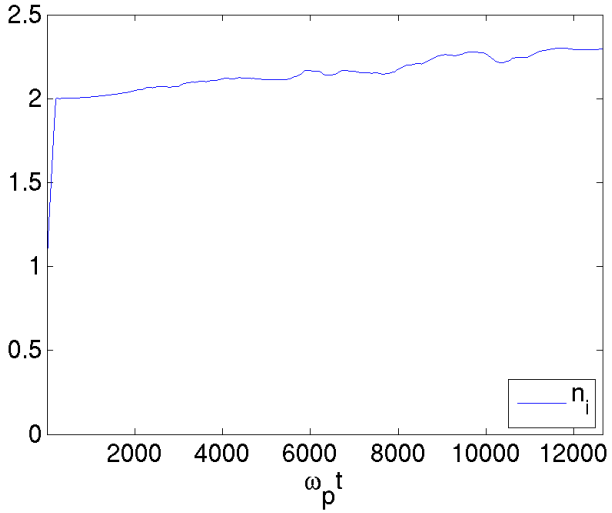

$\langle |a_{i+}| \rangle$ over $x = L_x/2 \pm 80$

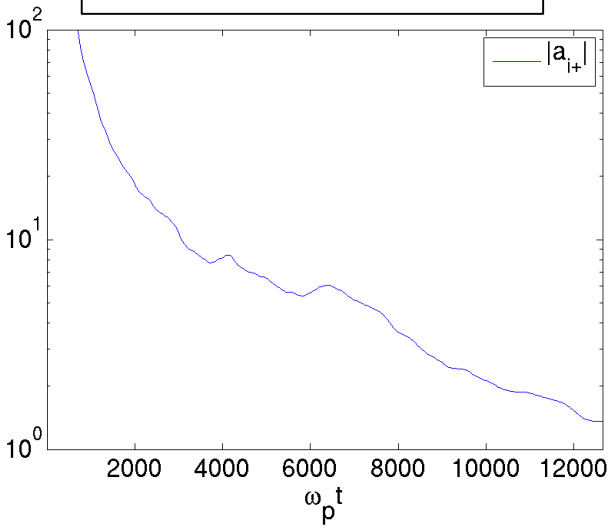

$\langle K_{ix+} \rangle, \langle T_{iy+} \rangle$ over $x = L_x/2 \pm 80$

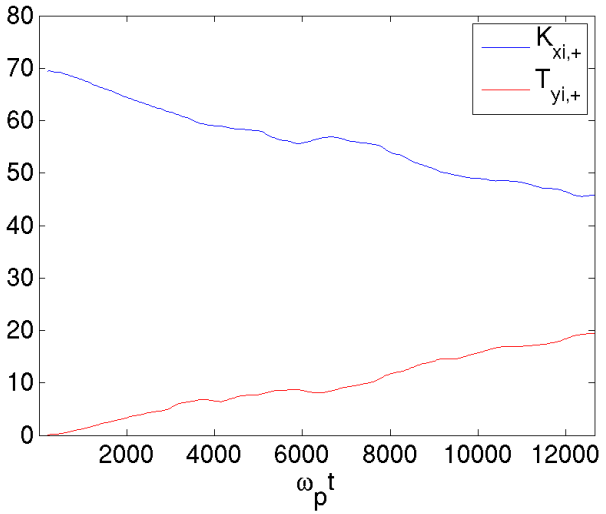

The incoming cold ions undergo strong pinching in contrast to the hotter transmitted ions

Density of the $+x$ injected ions

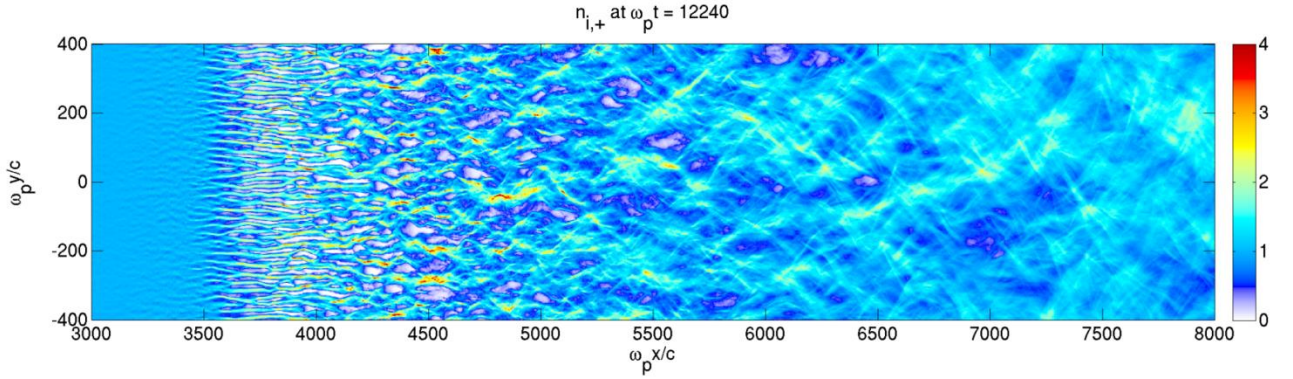

Density of the $-x$ moving ions

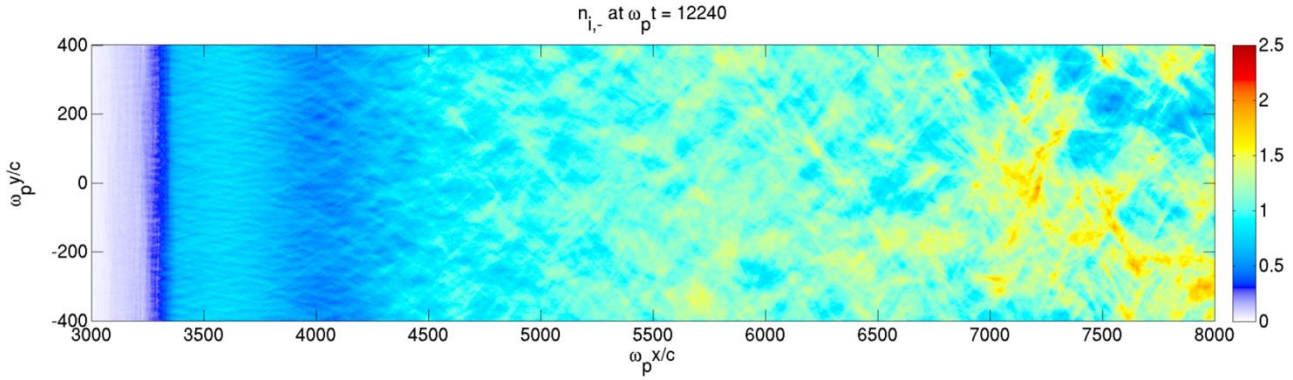

Magnetic field $eB_z/m_e\omega_p$

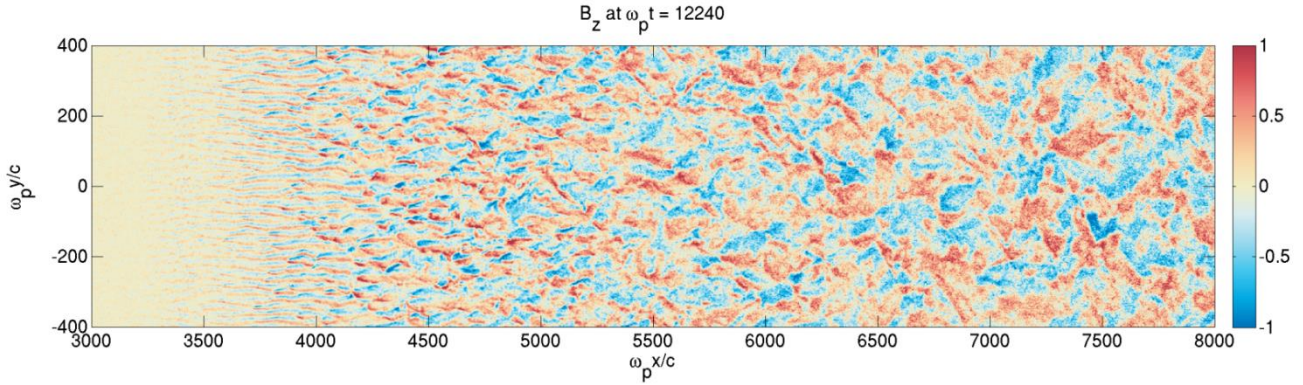

The incoming cold ions undergo strong pinching in contrast to the hotter transmitted ions

$x - p_x$ phase space of the $+x$ injected ions

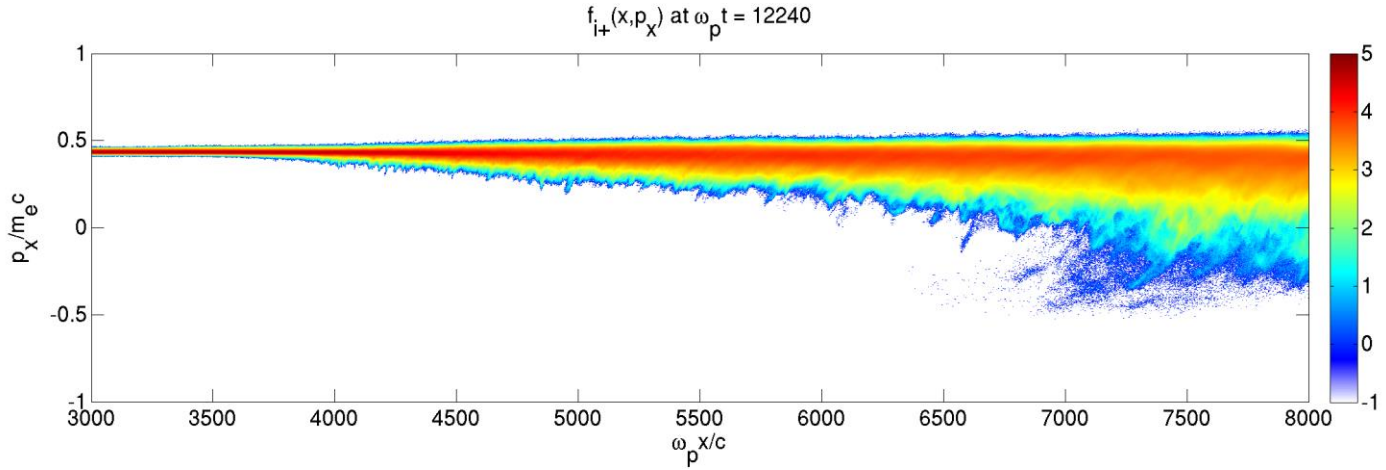

$x - p_x$ phase space of the $-x$ injected ions

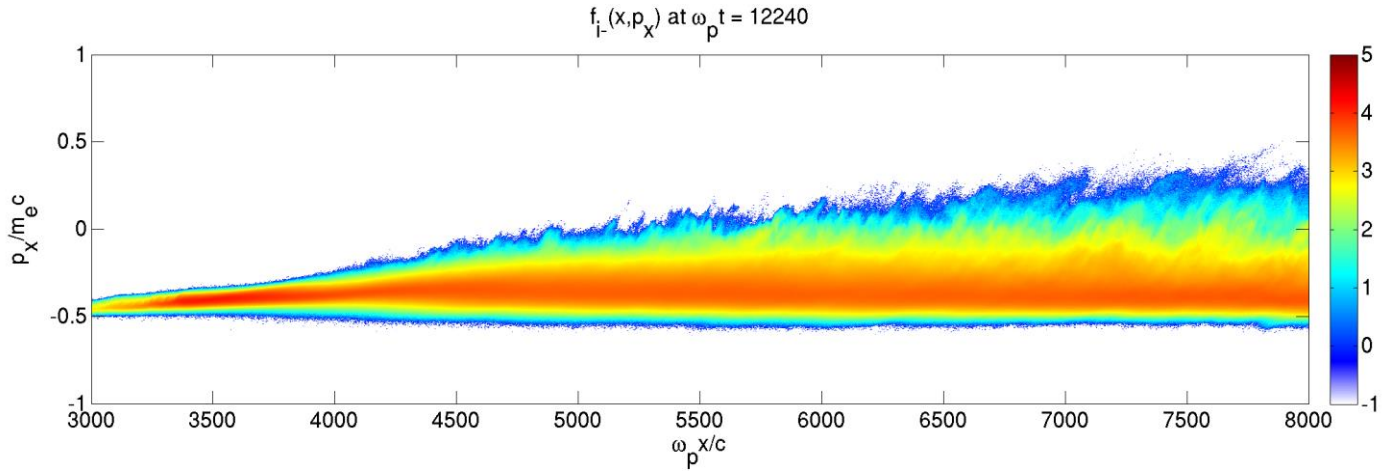

Transverse density and current density profiles at different locations in the upstream region

Current densities and B_z

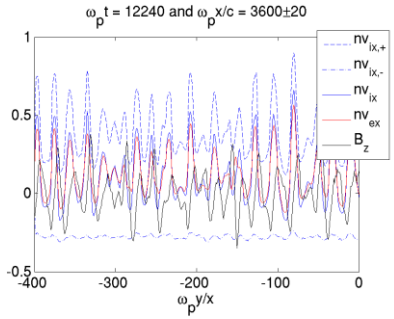

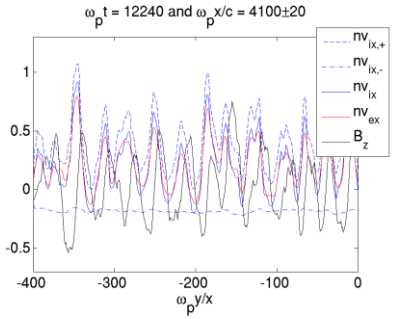

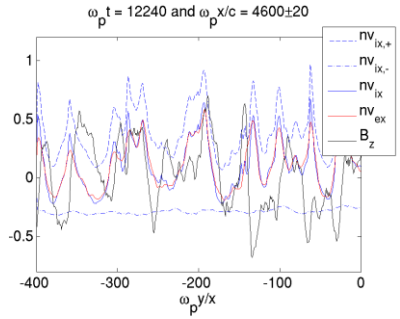

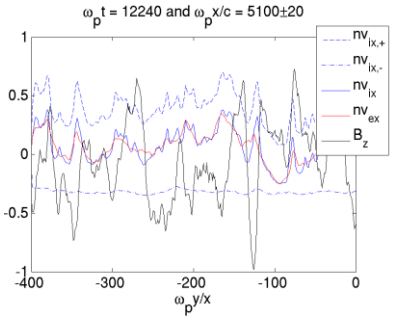

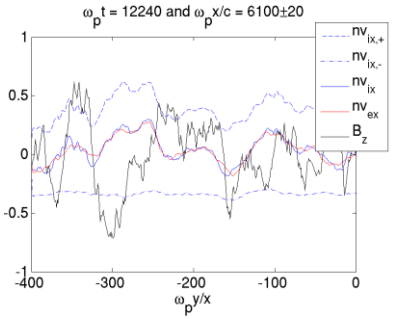

B_z and E_y

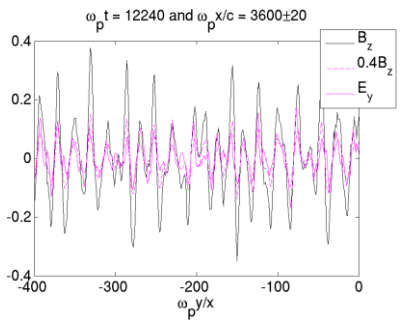

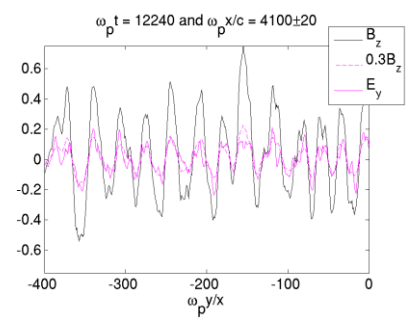

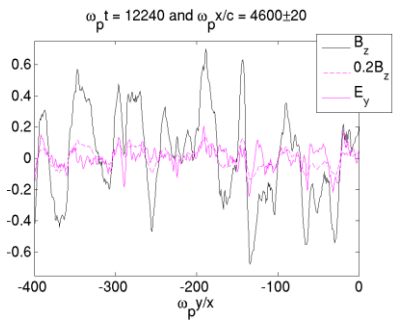

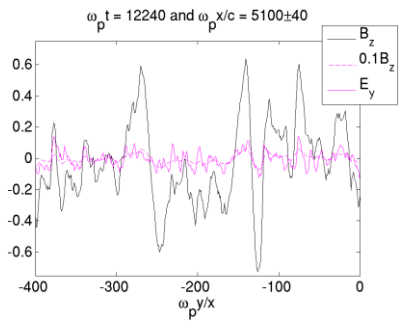

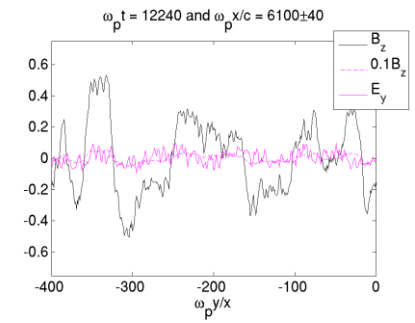

Mean velocity profiles of the $+x$ injected ions

x-velocity of the $+x$ injected ions

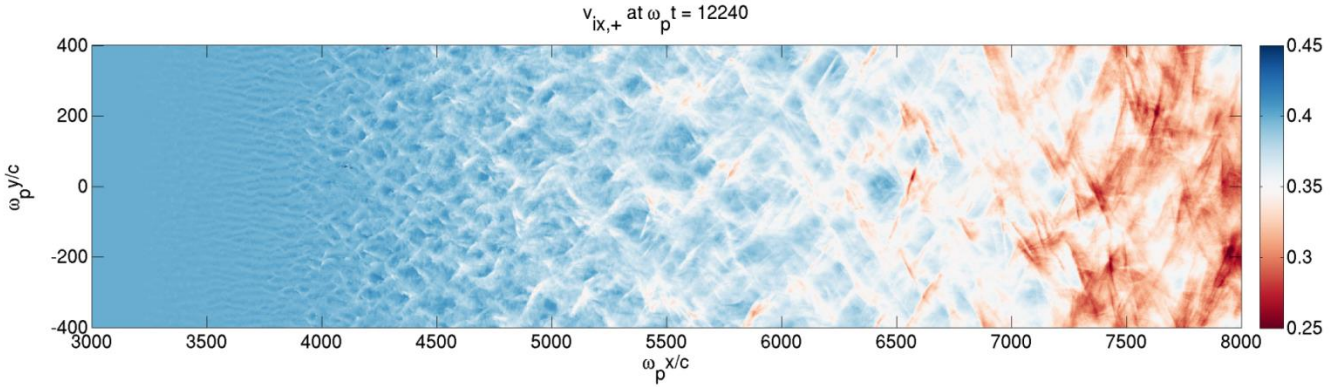

x-velocity of the $-x$ injected ions

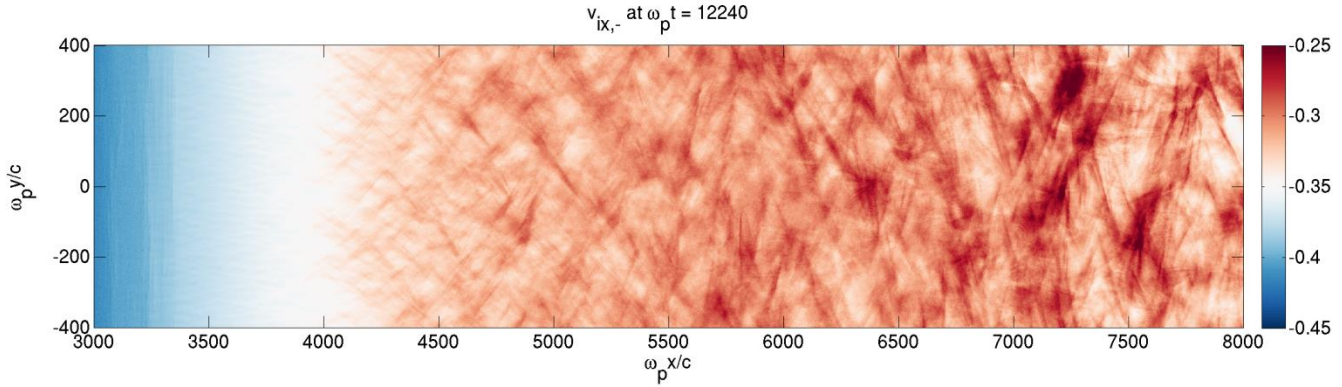

y-velocity of the $+x$ injected ions

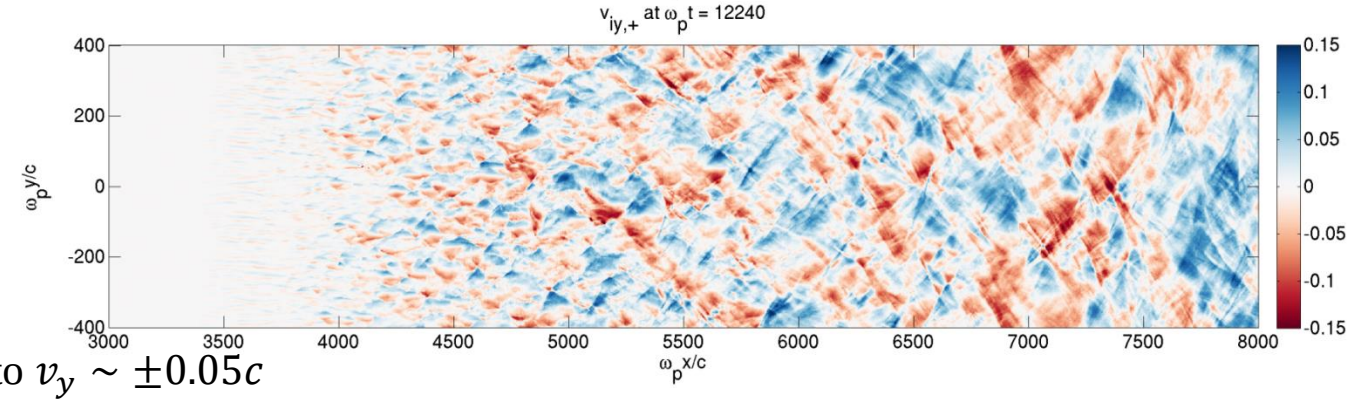

Filament decay corresponds to $v_y \sim \pm 0.05c$

Linear properties of Weibel modes (assumed purely electromagnetic) under various plasma conditions

Nonrelativistic linear theory in Weibel proper frame ($v_x = v_F$)

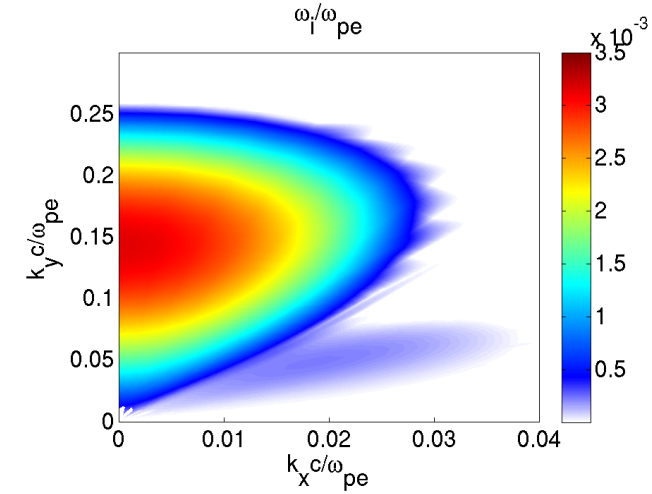

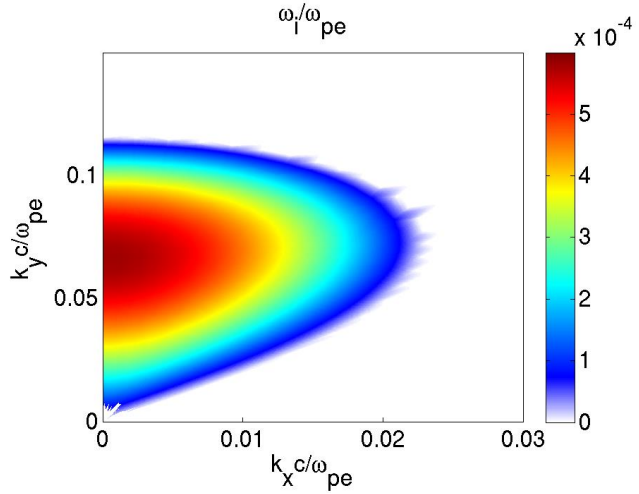

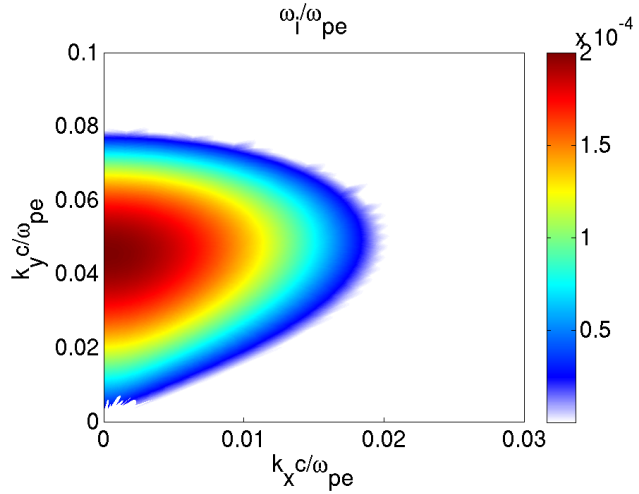

$= 0.4, n_{\pm} = 0.5, T_+ = 1, T_- = 10, T_e = 1, v_F \sim 0.12$

$v_+ = 0.35, v_- = -0.3, n_{\pm} = 0.5, T_+ = 5, T_- = 15, T_e = 2, v_F \sim 0.06$

$v_+ = 0.33, v_- = -0.25, n_{\pm} = 0.5, T_+ = 10, T_- = 20, T$

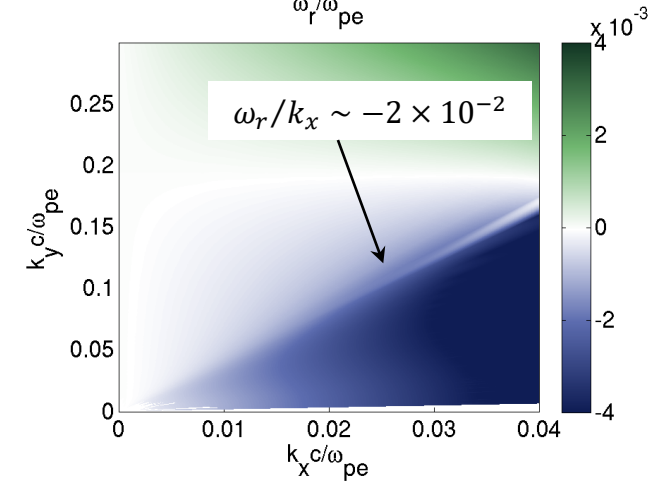

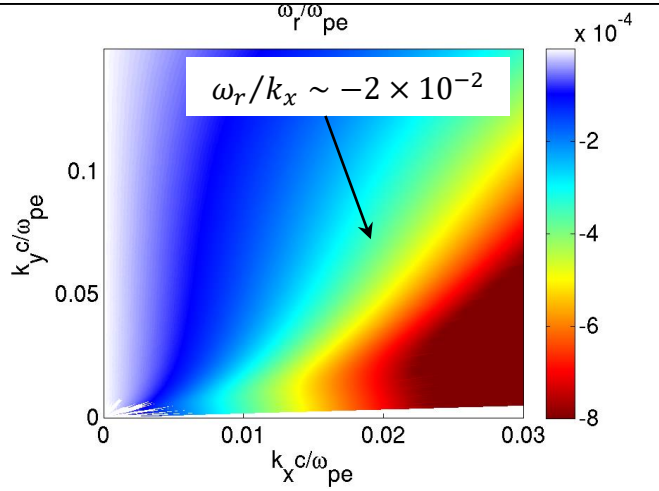

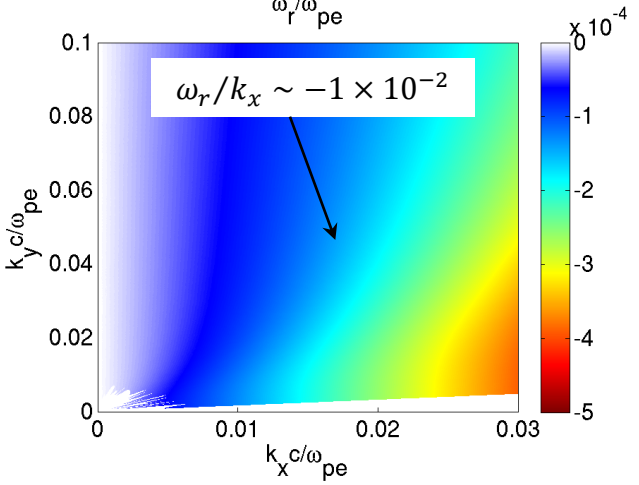

- We have $|\omega_{r,F}| \ll k_x v_{+,F} \equiv k_x(v_+ - v_F) \Rightarrow$ in the simulation frame, $\omega_r \sim k_x v_F \ll k_x v_+$

Mean electron & ion velocities

Velocity of $+x$ injected ions

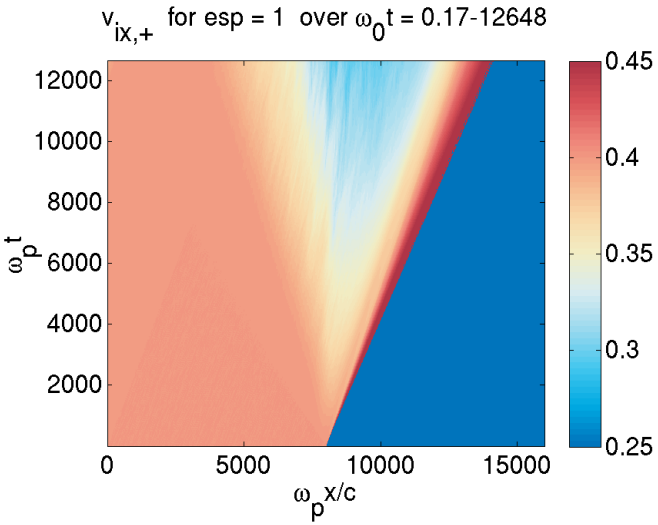

Velocity of $+x$ injected electrons

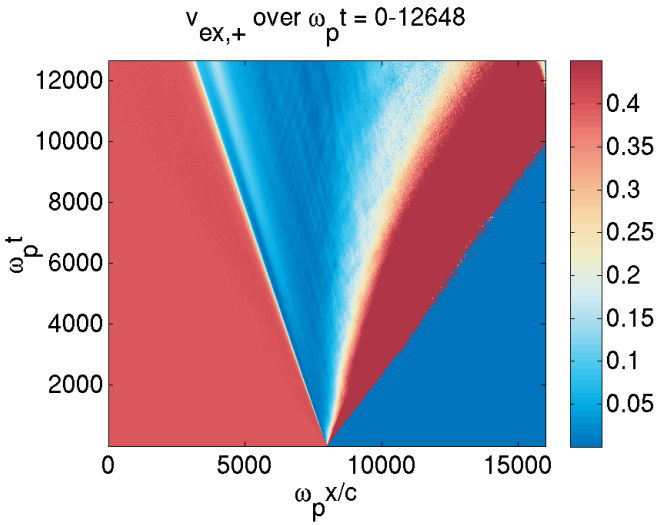

Mean electron velocity

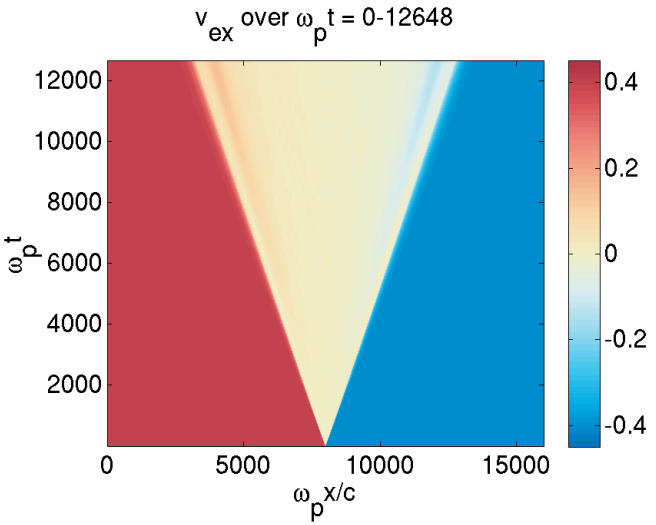

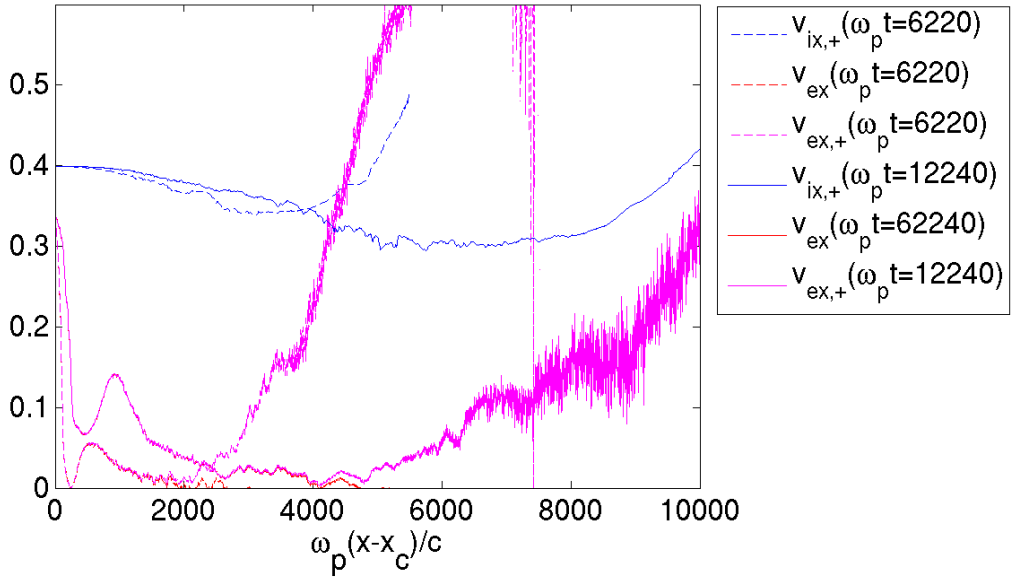

- Rapidly decreasing mean electron velocity
- $v_{ex,+} \sim v_{ex}$ holds up to the mid-plane.